MASARYKOVA UNIVERZITA
PŘÍRODOVĚDECKÁ FAKULTA
ÚSTAV BIOCHEMIE

STUDIUM EPITELIÁLNĚ-MEZENCHYMÁLNÍ TRANZICE NA BUNĚČNÝCH MODELECH RENÁLNÍHO KARCINOMU

Diplomová práce

Táňa Macháčková

Vedoucí práce: doc. RNDr. Ondřej Slabý, Ph.D. **Brno 2016**

Bibliografický záznam

Autor:	Táňa Macháčková Přírodovědecká fakulta, Masarykova univerzita Ústav biochemie
Název práce:	Studium epiteliálně-mezenchymální tranzice na buněčných modelech renálního karcinomu
Studijní program:	Biochemie
Studijní obor:	Analytická biochemie
Vedoucí práce:	doc. RNDr. Ondřej Slabý, Ph.D.
Akademický rok:	2015/2016
Počet stran:	75
Klíčová slova:	renální karcinom; epiteliálně-mezenchymální tranzice; mikroRNA

Bibliographic Entry

Author:	Táňa Macháčková Faculty of Science, Masaryk University Department of Biochemistry
Title of Thesis:	Study of epithelial-mesenchymal transition on cellular models of renal cell carcinoma
Degree programme:	Biochemistry
Field of Study:	Analytical Biochemistry
Supervisor:	Assoc. Prof. RNDr. Ondřej Slabý, Ph.D.
Academic Year:	2015/2016
Number of Pages:	75
Keywords:	renal cell carcinoma; epithelial-mesenchymal transition; microRNA

Abstrakt

Renální karcinom je nejčastějším nádorovým onemocněním ledvinného parenchymu a představuje přibližně 3 % všech zhoubných nádorových onemocnění dospělé populace. Renální karcinom se vyznačuje vysokou chemo- a radio-rezistencí a časným relapsem po nefrektomii. Jedním z klíčových procesů v progresi renálního karcinomu je proces epiteliálně-mezenchymální tranzice, který je zodpovědný za přeměnu nemotilních a neinvazivních epiteliálních buněk na motilní a invazivní mezenchymální buňky. MikroRNA jsou 18-25 nukleotidů dlouhé nekódující RNA schopné post-transkripční regulace genové exprese a jejich deregulace je spojena i s procesem epiteliálně-mezenchymální tranzice u renálního karcinomu.

Cílem této studie bylo ověřit účinky miR-429 *in vitro*. Jednalo se o sérii experimentů založených na *in vitro* indukci epiteliálně-mezenchymální tranzice u stabilních buněčných linií odvozených od renálního karcinomu. V průběhu experimentů byla sledována exprese epiteliálně-mezenchymálních markerů a to zejména E-kadherinu.

Abstract

Renal cell carcinoma is the most common neoplasm of renal parenchyma that accounts for about 3 % of all adult malignancies. Renal cell carcinoma is highly chemo- and radio-resistant tumour with occurence of early relapse after nephrectomy. Process of epithelial-mesenchymal transition plays crucial role during progression of renal cell carcinoma. Epithelial-mesenchymal transition is responsible for conversion of non-motile and non-invasive epithelial cells to motile and invasive mesenchymal cells. MicroRNAs are 18-25 nucleotides long non-coding RNAs which function in post-transcriptional regulation of gene expression. Deregulation of miRNA expression was also observed during epithelial-mesenchymal transition in renal cell carcinoma.

The goal of this study was to evaluate effects of miR-429 *in vitro*. We performed series of experiments based on *in vitro* induction of epithelial-mesenchymal transition in stable cell lines derived from renal cell carcinoma. Expression levels of epithelial-mesenchymal markers, especially E-cadherin, were observed during experiments.

MASARYKOVA UNIVERZITA
Přírodovědecká fakulta

ZADÁNÍ DIPLOMOVÉ PRÁCE

Akademický rok: 2014/2015

Ústav: Ústav biochemie

Studentka: Bc. Táňa Macháčková

Program: Biochemie

Obor: Analytická biochemie

Ředitel *Ústavu biochemie* PřF MU Vám ve smyslu Studijního a zkušebního řádu MU určuje diplomovou práci s tématem:

Téma práce: Studium epiteliálně-mezenchymální tranzice na buněčných modelech renálního karcinomu

Téma práce anglicky: Study of epithelial-mesenchymal transition on cellular models of renal cell carcinoma

Oficiální zadání:
Renální karcinom je nejčastějším nádorovým onemocněním ledvinného parenchymu a představuje přibližně 3 % zhoubných nádorů dospělé populace. Z urologických malignit dosahuje nejvyšší letality. Jedním z klíčových okamžiků v patogenezi nádorových onemocnění, včetně renálního karcinomu, je proces epiteliálně-mezenchymální tranzice (EMT). V rámci EMT dochází k přeměně epiteliálních buněk na více motilní a invazivní buňky mezenchymální. Narušená regulace exprese mikroRNA (miRNA) je jednou z kauzálních událostí v kancerogenezi a získávání invazivních vlastností RCC a specifické deregulace miRNA byly popsány i v souvislosti s procesem EMT u RCC. Cílem této práce bude série experimentů založených na in vitro indukci EMT u stabilních buněčných linií odvozených od RCC. Dalším cílem je analyzovat případné změny hladin exprese miRNA ovlivňujících tento proces (miR-200b, miR-200c, miR-141, miR-192 a miR-215). Součástí práce bude také měření exprese epiteliálních a mezenchymálních markerů (ZEB1, ZEB2, E-kadherin, N-kadherin, vimentin).

Jazyk závěrečné práce: angličtina

Vedoucí práce: doc. RNDr. Ondřej Slabý, Ph.D.

Datum zadání práce: 14. 10. 2014

V Brně dne: 27. 11. 2014

Souhlasím se zadáním (podpis, datum):

Bc. Táňa Macháčková **studentka**	doc. RNDr. Ondřej Slabý, Ph.D. **vedoucí práce**	doc. RNDr. Oldřich Janiczek, CSc. **zástupce ředitele Ústavu biochemie pro pedagogické záležitosti**

Poděkování

Na tomto místě bych ráda poděkovala vedoucímu své diplomové práce doc. RNDr. Ondřeji Slabému, Ph.D. za odborné vedení, cenné připomínky a vstřícný přístup. Dále děkuji své odborné konzultantce Mgr. Haně Mlčochové za vedení při práci v laboratoři po celou dobu mého studia, trpělivost a korekci práce. Za rady ohledně statistického zpracování dat děkuji Mgr. Jaroslavu Juráčkovi. Na závěr bych ráda poděkovala celému kolektivu skupiny Molekulární onkologie II-solidní nádory za podporu a přátelskou atmosféru.

Prohlášení

Prohlašuji, že jsem svoji diplomovou práci vypracovala samostatně s využitím informačních zdrojů, které jsou v práci citovány.

Brno 12. května 2016 ……

Táňa Macháčková

Table of contents

List of abbreviations

3'UTR	Three prime untranslated region
AGO	Argonaute protein
BC	Breast carcinoma
BMP	Bone morphogenic protein
ccRCC	Clear cell renal cell carcinoma
ChRCC	Chromophobe renal cell carcinoma
CRC	Colorectal carcinoma
CSC	Cancer stem cell
Ct	Cycle threshold
DGCR8	DiGeorge Syndrome Critical Region Gene 8
DNA	Deoxyribonucleic acid
dsRNA	Double strand ribonucleic acid
ECM	Extracellular matrix
EMT	Epithelial-mesenchymal transition
EMT-TF	Epithelial-mesenchymal transition associated transcription factor
EPO	Erythropoietin
HIF1	Hypoxia-inducible factor 1
LOH	Loss of heterozygosity
MET	Mesenchymal-epithelial transition
MDR1	Multidrug ressistance protein 1
miRISC	MicroRNA-induced silencing complex

mRNA	Mediator ribonucleic acid
miRBase	MicroRNA database
miRNA	MicroRNA
miR	MicroRNA
MRE	MiRNA recognition element
MTT	3-(4,5-dimethylthiazol-2-yl)-2,5-diphenyltetrazolium bromide
MYC	Myelocytomatosis oncogene
ncRNA	Non-coding ribonucleic acid
NSCLC	Non-small cell lung cancer
p53	Tumour protein 53
PDGF	Platelet derived growth factor
PPIA	Peptidylprolyl isomerase A
pRCC	Papillary renal cell carcinoma
pre-miRNA	Precursor miRNA
pri-miRNA	Primary miRNA
PTM	Post translation modification
pVHL	Von Hippel-Lindau protein
qRT-PCR	Quantitative real time polymerase chain reaction
RBM	RNA binding motif
RCC	Renal cell carcinoma
RNA	Ribonucleic acid
RNApolII	RNA polymerase II
RT	Reverse transcription

TF	Transcription factor
TGF	Transforming growth factor
TLDA	TaqMan Low Density Arrays
TRBP	TAR RNA binding protein
VEGF	Vascular endothelial growth factor
VHL	Von Hippel-Lindau syndrome
VHL	Von Hippel-Lindau gene
Wnt	Wingless-type MMTV integration site family
XPO5	Exportin 5
ZEB1	Zinc finger E-box binding homebox 1
ZEB2	Zinc finger E-box binding hmebox 2
ZFC	Zinc finger cluster

Introduction

Renal cell carcinoma is the most common urological cancer that accounts for about 3% of all adult malignancies. This type of cancer is specific by its high chemo- and radio-resistance and high risk of relapse after surgical treatment. All patients with RCC undergo total or partial resection of the kidney with the tumor. Unfortunately, about 40% of all RCC patients experience recurrence of the disease, even after this radical intervention. This could be happening due to presence of process called epithelial-mesenchymal transition. Epithelial-mesenchymal transition is a biological process that allows a cell of an epithelial phenotype change to a cell of a mesenchymal phenotype. Mesenchymal phenotype is connected to higher motility and invasivness of the cells and it is initial step of the metastatic cascade. The transition is driven by many molecules and microRNAs are one of them.

Since the discovery of non-coding RNAs and the fact that they have important role in regulation of gene expression, number of studies about this topic has grown continually. Deregulation of microRNAs is often associated with various diseases and cancers. Between microRNAs involved in regulation of epithelial-mesenchymal transition are the most described miRNAs that belong to miR-200 family. Members of miR-200 family (miR-200a, miR-200b, miR-200c, miR-141 and miR-429) cooperatively regulate translation of E-cadherin transcriptional repressors ZEB1 and ZEB2. These microRNAs often create regulation loops with their targets so they can function like molecular on-off switches.

The aim of this diploma thesis was to evaluate impact of microRNA-429 on process of epithelial-mesenchymal transition in stable cell lines derived from RCC. This was done by *in vitro* induction of epithelial-mesenchymal transition using transforming growth factor β followed by functional analyses.

1. Theoretical part

1.1 Renal cell carcinoma

Kidney and renal pelvis cancer ranges between top ten most common cancers in the world. The most frequent type of renal neoplasm is renal cell carcinoma (RCC), which accounts for 85% of all renal malignancies. This malignity arises from the various parts of the nephron and can be classified into several subtypes [1]. The most common subtype is clear cell renal cell carcinoma (ccRCC), (70%) followed by less common papillary renal cell carcinoma (pRCC), (10-15%) and chromophobe renal cell carcinoma (ChRCC), (5%), [2]. These subtypes differ not only histologically but they also have different clinical features and genetic determinants [3].

1.1.1 Incidence

Incidence of RCC varies internationally and Czech Republic ranks with the highest incidence of RCC in the world (22/100,000 in men and 9.9/100,000 in women), (Figure 1). Developed countries have higher incidence than less developed [4]. This fact could be caused by higher chance of incidental diagnosis of RCC due to better technique in developed countries and risk factors connected with western society [2].

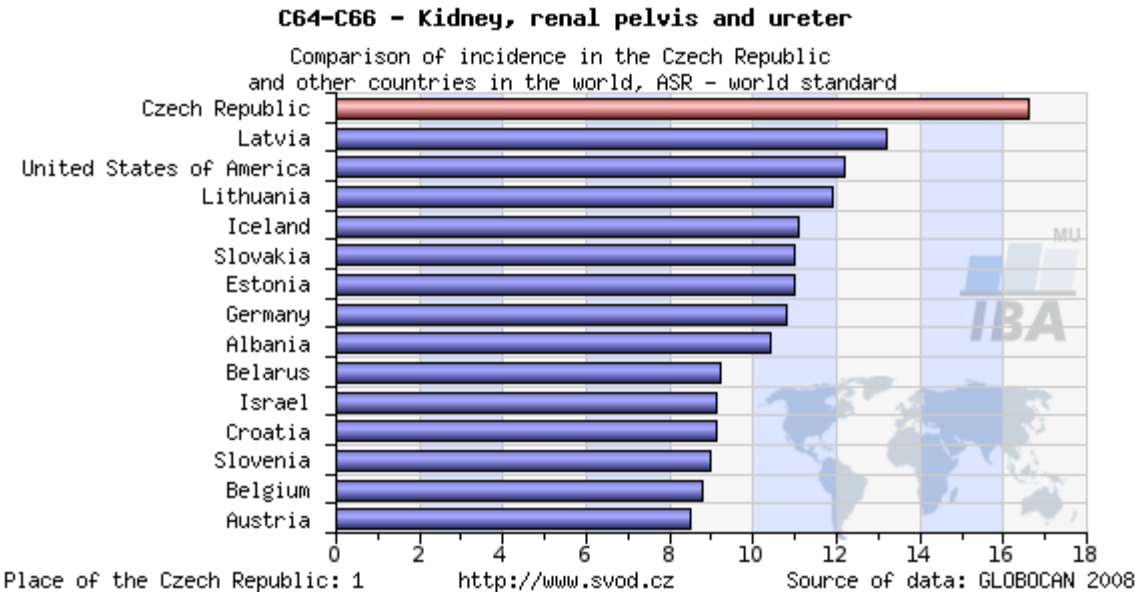

Figure 1: Comparison of incidence in the Czech Republic and other countries [4].

1.1.2 Mortality

Over the decades mortality rate decreased. Cause of this phenomenon is probably improvement of detection techniques. This improvement leads to a higher chance of incidental diagnosis and diagnosis at early stages of RCC. In contrast to that, incidence rate increases (Figure 2). However, mortality rate between countries varies and there is no satisfactory explanation for this fact till today [5].

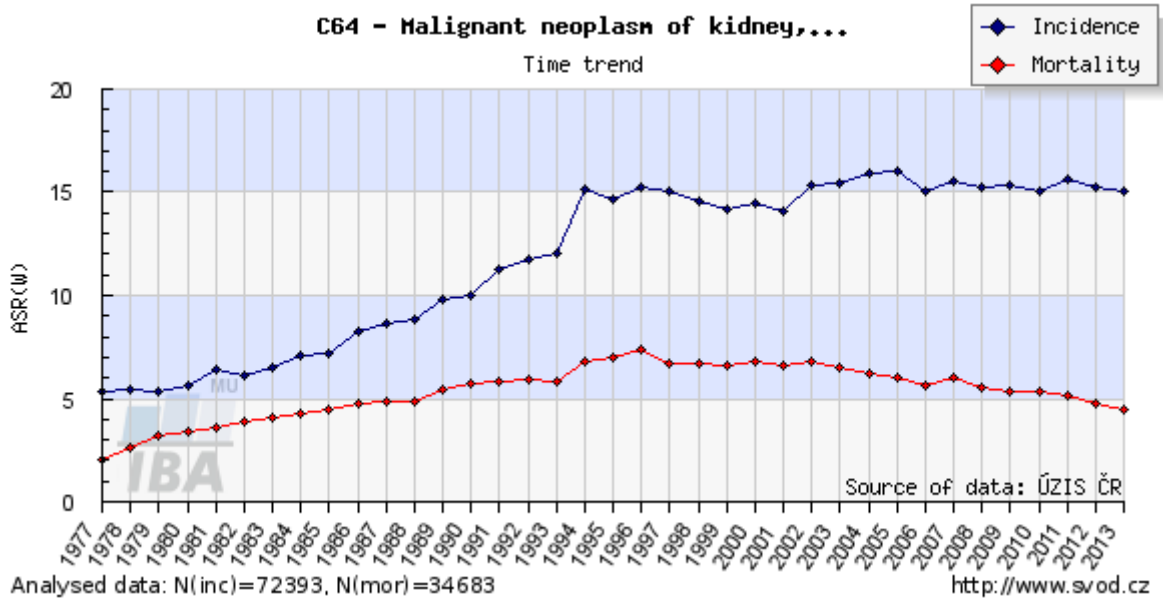

Figure 2: Incidence and mortality of RCC in the Czech Republic 1977-2013 [4].

1.1.3 Risk factors

Based on the current observations - smoking, obesity, and hypertension are the most well-estabilished risk factors for developing RCC. From the evidence, tobacco exposure is the biggest risk factor. There are multiple mechanisms that describe how smoking promotes development of RCC. Cigarette smoke induces oxidative stress and injury in the kidney and causes renal impairment. Also the free radicals contained in cigarette smoke cause oxidative DNA damage, which may lead to the development of cancer [2,6]. Several studies have demonstrated an increased risk for RCC in association with obesity [5].

1.1.4 Sex and Age

RCC is globally as twice as common in males as in females. Age also plays role in incidence. Occurence of RCC increases rapidly after fifth decade of life [4].

1.1.5 Pathogenesis of clear cell renal cell carcinoma

Clear cell renal cell carcinoma is the most common subtype of RCC and accounts for 70% of all RCCs. Cells of the ccRCC appear translucent under the microscope and this is how this subtype got its name. RCC is mostly sporadic tumor but there are also several hereditary and familial forms. The most described is the Von-Hippel Lindau (VHL) syndrome. VHL syndrome is associated with occurrence of ccRCC, hemangiomas and pancreatic tumours. The *VHL* gene is an evolutionarily well conserved tumour-suppressor gene composed of at least three exons [7]. Product of *VHL* gene is VHL protein (pVHL) that plays important role in regulation of hypoxia pathway. The *VHL* protein (pVHL) functions as a part of an E3 ubiquitin ligase which ubiquitylates protein called Hypoxia Inducible Factor 1 (HIF1) and targets this protein for degradation by proteasome. This complex is consisted of elongin B, elongin C, cullin and pVHL. HIF is a heterodimeric protein which consist of two subunits (HIF-α and HIF-β) and plays major role in cellular response to oxidative stress. Early event in ccRCC pathogenesis is a loss of *VHL* gene function due to its deletion on chromosome 3p, loss of heterozygosity (LOH), promoter methylation or missense mutation. The lack of functional pVHL or low concentration of oxygen cause that subunits of HIF can translocate to the nucleus and function as transcriptional factors. HIF proteins transcriptionally target and promote expression of many oncogenic molecules including Vascular Endothelial Factor (VEGF), Platelet Dervied Growth Factor (PDGF), Multidrug Resistance Protein 1 (MDR-1) and Erythropoietin (EPO), (Figure 3), [8,9]. Mutation, loss or methylation of both *VHL* alleles, has been reported in sporadic ccRCC and in the inherited *VHL* syndrome [9]. Additionally, hypoxia and HIF-α are linked to transcriptional factor TWIST. Upregulation of TWIST cause higher expression of pro-EMT molecules and supports promotion of EMT. The kidney is mesenchymal in origin and develops through mesenchymal-epithelial transition. In ccRCC this transition is reversed and results in EMT and dedifferentation. This transition requires presence of transcription factors like Snail, Slug, ZEB1 and ZEB2 [10].

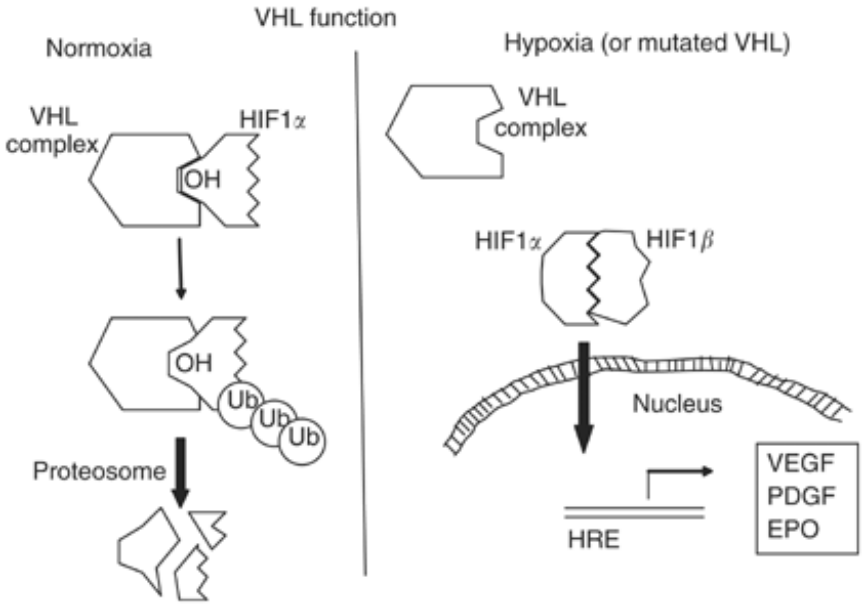

Figure 3: Function of VHL protein [11].

1.2 Epithelial-mesenchymal transition

Epithelial mesenchymal transition is a biologic process that allows cells of epithelial phenotype to undergo series of biochemical processes that result in mesenchymal phenotype. Mesenchymal phenotype includes enhanced migratory capacity, invasivness, elevated resistance to apoptosis and increased production of extracellular matrix (ECM) components. Characteristic event during EMT is a loss of E-cadherin and its replacement by another type of cadherin. This process is called cadherin switch. With the loss of E-cadherin expression of mesenchymal markers increases. The most well known EMT markers are vimentin, fibronectin, ZEB1, ZEB2, Snail, Slug, Twist, N-cadherin, E-cadherin, zonula occludens and clusterin [12,13].

1.2.1 Types of EMT

Process of EMT is mainly associated with embryonic development and organ formation. However, EMT dysfunction in normal cells leads to diseases such as cancer and fibrosis. EMT occurs in three different biological settings - embryogenesis, organ fibrosis and carcinogenesis (Figure 4), [14].

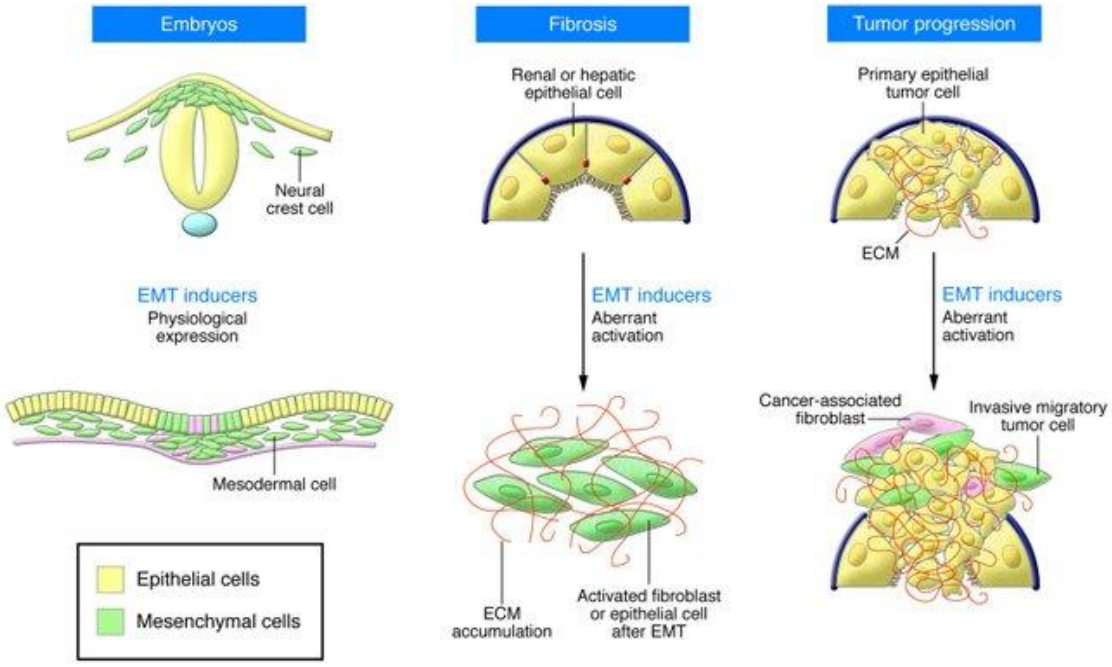

Figure 4: Types of epithelial-mesenchymal transition [12].

During embryogenesis EMT plays a critical role in generating the first set of mesenchymal cells, which are known as the primary mesenchyme. This primary mesenchyme gives rise to a secondary epithelia via mesenchymal-epithelial transition (MET). Whole process of organ formation during embryogenesis is dependent on EMT and MET [15].

Fibrosis or scarring is a feature of many chronic inflammatory diseases. This process is characterized by overexpression of ECM components which results in tissue scarring. Epithelial tissue has ability to heal itself after trauma by generating cells of mesenchymal phenotype and activation of fibroblasts. Mesenchymal cells can generate components of ECM, molecules important for healing. In healthy organism production of mesenchymal cells stops when the tissue is healed. In organism affected by fibrosis production of these cells lasts and results in total destruction of function and structure of the tissue. This production of mesenchymal-like cells from epithelial tissue is possible due to EMT [16].

Third type of EMT is associated with carcinogenesis. Cells of carcinomas generated by EMT lose apical-basal polarity, connection to basal lamina and to each other, and achieve mesenchymal features as enhanced migratory capacity, invasivness, resistance to apoptosis, ability to escape from immune system and expression of metalloproteinases.

Cells with mesenchymal features are capable of degradation of ECM, intravassation and extravassation followed by MET and thus formate secondary tumour (Figure 5). There are two hypotheses that are trying to explain EMT and metastasis. In the first hypothesis cancer progenitor cells present in a tumour do not undergo EMT simultaneously, so the cancerous population contains cells at different stages of differentiation. Cancer progenitor cells can undergo EMT to achieve further stage of differentation and develop into advanced stage of cancer. Although these grades are different, they arise from the same progenitor cell and undergo differential EMT at different time points. The second hypothesis predicts cancer progenitor cells to undergo EMT and then metastatize following by clonal expansion [17]. EMT is also considered as a process capable of generating cancer stem cells (CSCs). Last step of metastasis is adaptation and colonisation of foreign tissue by cancer cells. It seems unlikely that these adapative steps are enabled only by EMT programs and thus may require additional changes to cells. It seems that the most important of these adaptive changes is self-renewal. Self-renewal enables progenitor cell to generate cells that are copies of itself. CSCs possess this ability of self-renewal and are linked to many different types of cancer [18].

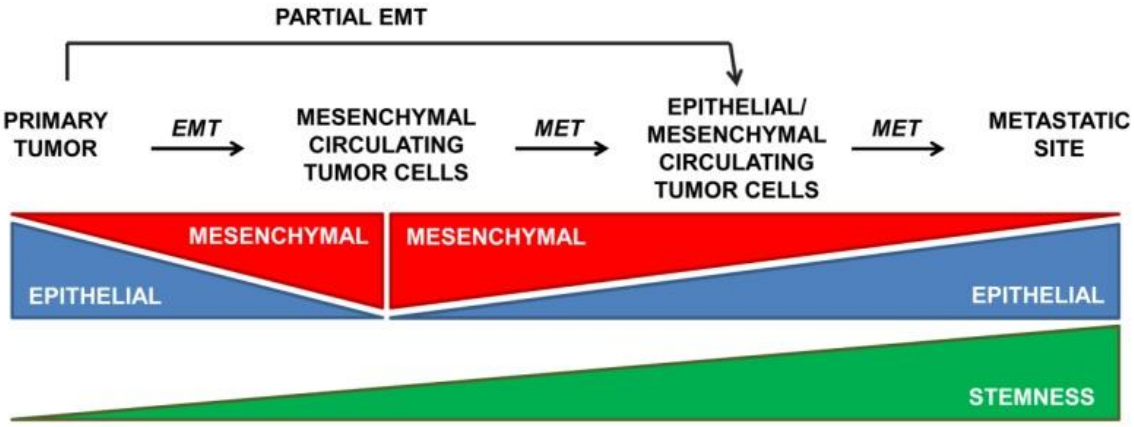

Figure 5: EMT, MET and stemness during carcinogenesis [19].

1.2.2 E-cadherin

Epithelial cells display cell to cell adhesions, adhesions to ECM and apical-basal polarity. Cell to cell adhesions are realised through adherens junctions, tight junctions, gap junctions and desmosomes at lateral surfaces. Apical-basal polarity is maintained due to connection of cells to basal lamina. During EMT these juncions are deconstructed and

junction proteins are relocalised or degradated. E-cadherin is one of the most important proteins in cell to cell adhesion and EMT initiation is accompanied by decrease of E-cadherin expression. Both EMT and MET are dependent on E-cadherin expression levels. E-cadherin is a calcium-dependent homodimeric transmembrane glycoprotein present in epithelial cells and can be regulated on both mRNA and protein levels [20]. E-cadherin ectodomains are linked to actin cytoskeleton by α-catenine and β-catenine and its endodomains bind homotypically with each other via Ca^{2+} bridges (Figure 6).

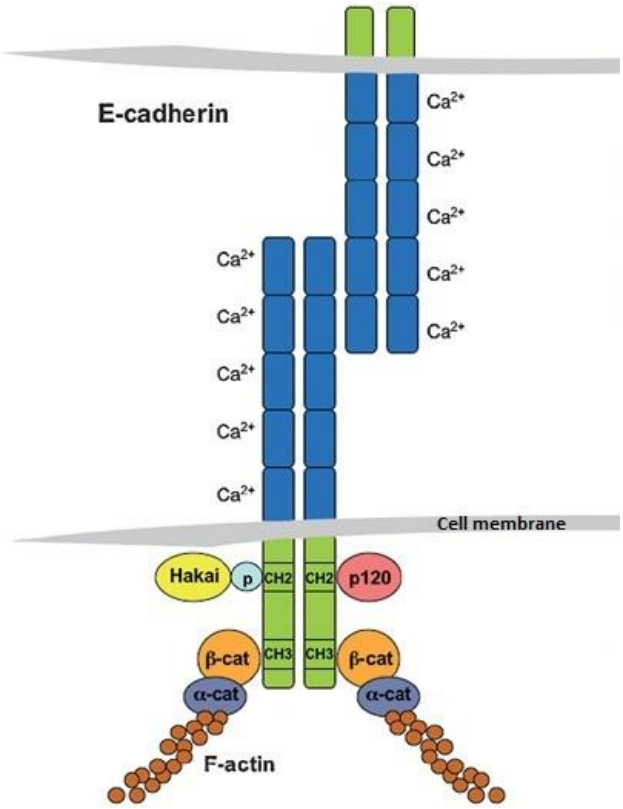

Figure 6: Adherens junction represented by E-cadherin homotypical binding [21].

Cells undergoing EMT often present switch from E-cadherin to another type of cadherin. Mesenchymal cells express various types of cadherins including N-cadherin, R-cadherin and cadherin-11. It is well known that cadherin switching allows cells to segregate population of cells from their neighbours by expression of certain type of cadherin. However, there is no satisfactory explanation of how cadherin switch promotes migratory capacity and invasivness which are essential for metastasis. There are three potential underlying mechanisms: the capacity of E-cadherin to regulate β-catenin signaling in the canonical Wnt pathway, its potential to inhibit mitogenic signaling through growth factor receptors and the possible links between cadherins and the

molecular determinants of epithelial polarity. The term cadherin switching usually refers to a switch from E-cadherin to N-cadherin [22,23].

1.2.3 Cytoskeleton rearrangement

The cell cortex is composed of microfilament cytoskeleton, microtubule network and intermediate filaments. Microfilament cytoskeletone influeneces cell morphology, migration capacity and invasivness. Microtubule network is the driving force of cell migration. In epithelial cells intermediate filaments are at least ten times more abundant than microfilaments and microtubules, and their main role is to reinforce cells and to reorganize cells into tissue. It is clear that rearrangement of epithelial cytoskeleton is necessary during EMT [24].

1.2.4 Regulation of EMT

EMT is regulated at several levels. At transcriptional level by wide range of transcriptional factors (TFs), at post-transcriptional level by non-coding RNAs and at post-translational level by post-translational modifications (PTMs). Transcriptional regulation is initiated by microenvironmental (hypoxia) or/and biological factors (transforming growth factor (TGF), bone morphogenic protein (BMP)) and is orchestrated by a network of EMT associated transcription factors (EMT-TFs) that interact with epigenetic regulators to control the expression of proteins involved in cell to cell connection, ECM degradation and cytoskeleton rearrangement. E-cadherin is a key molecule in EMT and its promotor is a target of majority of EMT-TFs [25]. There are three families of EMT-TFs that have central role in regulation of EMT - Snail, ZEB and TWIST (Figure 7). EMT-TFs have potential to transcriptionally repress expression of epithelial markers (e.g. E-cadherin, Occludin, Desmoplakin, Plakophilin and Zonula Occludens) and to enhance expression of mesenchymal markers (e.g. N-cadherin, α-smooth muscle actin, vimentin, fibronectin, vitronectin). Funciton of these TFs is further enhanced by close cooperation with the epigenetic machinery [26,27]. Transcription factors from Snail family are zinc-fnger TFs and are capable of direct repression of *E-cadherin* transcription. The most well known TFs from Snail family are Snail encoded by *SNAI1* gene and Slug encoded by *SNAI2* gene [28]. ZEB family includes two zinc-finger transcription factors known under names zinc finger E-box binding homebox 1 (ZEB1)

and zinc finger E-box binding homebox 2 (ZEB2). ZEB1 and ZEB2 function as E-cadherin repressors as well. Structurally are ZEB proteins comprised of two zinc finger clusters (ZFCs) located towards the N- and C- terminal ends of the protein. These zinc-finger motifs bind to ZEB boxes in the regulatory regions of target genes. Towards the centre of ZEB proteins there is an extra zinc finger that also helps to bind to the DNA. ZEB proteins are highly modular with independent regions mediating their binding to DNA, to other TFs and to proteins with activator or repressor activity but lacking a DNA binding motif on their own [29]. The TWIST family includes two members - Twist-1 known as Twist and Twist-2 known as Dermo-1. Both Twist and Dermo-1 are basic helix-loop-helix TFs that have important regulatory functions during embryo development. These proteins may function either as transcriptional activators or repressors through both direct and indirect mechanisms. Twist acts as an oncogene and is negatively associated with protein p53. High expression of Twist is correlated with numerous types of carcinomas, sarcomas, glioblastomas, neuroblastomas, and melanomas [30,31].

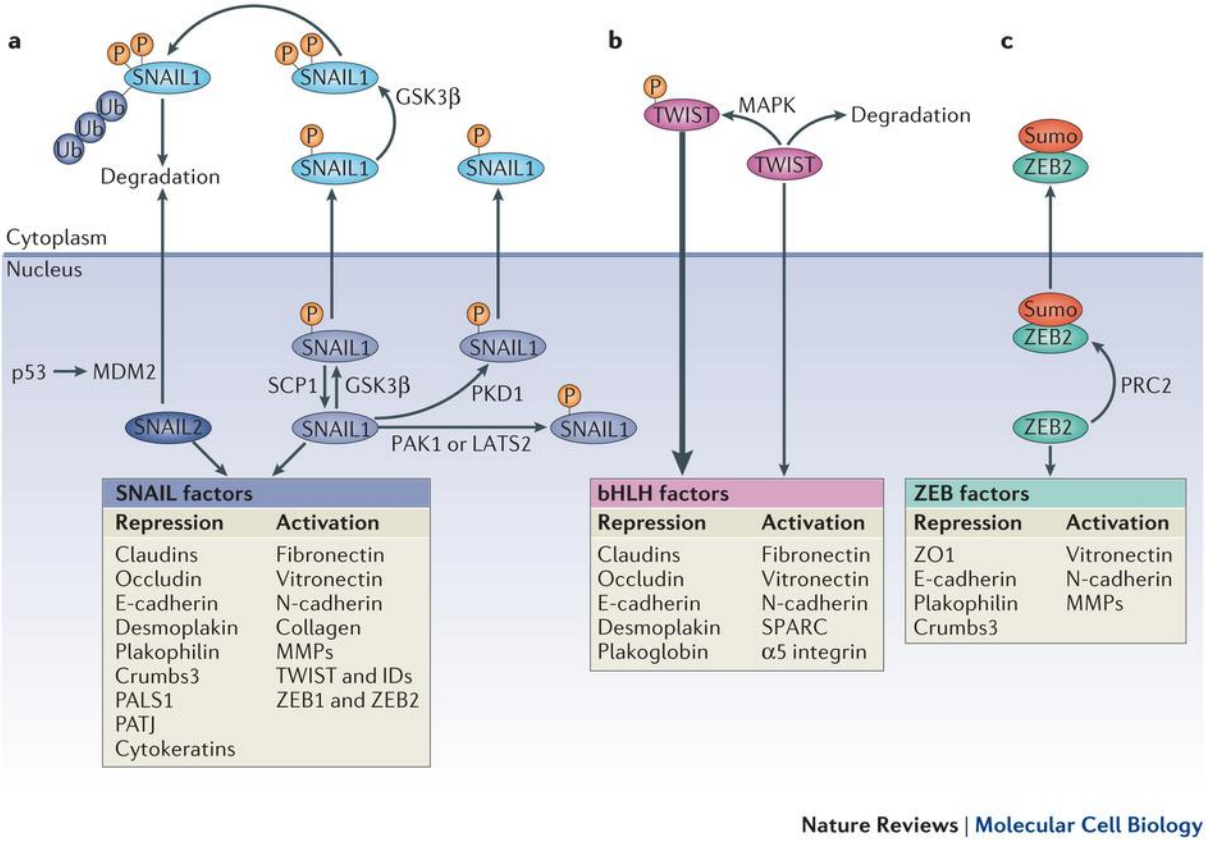

Figure 7: Transcription factors involved in EMT [26].

Post-transcriptional regulation of EMT is provided by microRNAs. The most well-known microRNAs involved in EMT regulation are members of miR-200 family. These miRNAs target mRNAs of EMT-TFs that repress E-cadherin and almost all of them are tumor suppressors. EMT-TFs and miRNAs often create reciprocal regulation loops. Post-translational modifications are covalent modificiations of a newly translated protein from mRNA. Protein is during PTMs modified by introduction of new functional groups into the peptide side amino acid chains. PTMs can either occur on a single residue or on multiple residues. Chemical modifications present during process of EMT include hydroxylation, phosphorylation, SUMOylation and glycosylation. PTMs can either have stabilisating or destabilisating effect on the modified protein [32].

1.3 MicroRNA

MicroRNAs (miRNAs) are a class of small non-coding RNAs that function as guide molecules in RNA silencing. They are approximately 18-25 nucleotides long and capable of post-transcriptional regulation of gene expression in metazoa and plants. At 5'termini miRNAs have 2-8 nucleotides long sequence that is essential for pairing with their targets. This sequence is called seed sequence and is complementary to the miRNA recognition elements (MREs) within 3' termini untranslated region (3'UTR) of mRNAs. MiRNAs act as guides by partial or perfect base pairing with they target mRNAs. These small RNAs are closely connected to Argonaute (AGO) family proteins. AGO proteins serve as effectors by recruiting factors that induce translational repression, mRNA deadenylation and mRNA decay [33].

1.3.1 MicroRNA biogenesis

MiRNA genes are localized through the whole genome including intronic, exonic and protein coding regions. In humans majority of miRNAs is encoded by introns of non-coding and coding transcripts. They are often present in clusters and are transcribed as polycistronic transcripts [34]. Their genes usually have their own promotors but if they arise from protein-coding gene, they can share promotor of the host gene. The latest release of the miRNA database (miRBase) has catalogued 2,588 genes for human miRNAs. The most accepted model of miRNA biogenesis is canonical biogenesis and it is predicted that majority of miRNAs is processed this way (Figure 8). According to the

cannonical biogenesis the miRNA genes are transcribed by Polymerase II (RNApolII) as long double strand RNA (dsRNA) primary transcripts called primary miRNA (pri-miRNA). Within long primary transcript is a local hairpin structure where miRNA sequences are embedded. Transcription is positively or negatively regulated by RNApolII-associated factors (p53, MYC, ZEB1, ZEB2) and epigenetic regulators (DNA methylation, histone modification), [33]. In the nucleus pri-miRNA is cleaved into 70 nucleotides long precursor-miRNA (pre-miRNA) by a complex of proteins. This complex is called microprocessor complex and is comprised of RNAseIII Drosha and dsRNA binding protein Pasha (DGCR8), [35]. Pre-miRNA structure is then exported to the cytoplasm, where undergoes another cleavage. The transport from the nucleus to the cytoplasm is carried by a karyopherin Exportin 5 (XPO5) and small Ran protein with GTPase activity. Cytoplasmic cleavage of stem loop structured pre-miRNA into 18-25 nucleotides long miRNA/miRNA* duplex is realised by RNAseIII Dicer and TAR RNA binding protein (TRBP). Consequently, miRNA/miRNA* duplex is divided into two separate strands. Leading strand (strand with less stable 5' termini) is incorporated into a complex of proteins and the other strand is degradated [36,37]. Leading strand of miRNA is called mature miRNA. This protein/miRNA complex is called microRNA induced silencing complex (miRISC). MiRISC complex consists of Argonaute proteins (AGO1-4), proteins GEMIN3 and GEMIN4 and mature miRNA. Incorporated miRNA is able to bind to the complementary sequences in 3'UTR of target mRNAs and thus initiate translational repression, deadenylation or degradation of mRNA. Translational repression, deadenylation and degradation is provided by proteins from miRISC complex. The fate of the mRNA depends on the degree of miRNA/mRNA hybridization and due to this one miRNA is able to target up to hundreds of mRNAs [33]. Canonical biogenesis pathway requires microprocessor complex for processing mature miRNA from pri-miRNA and pre-miRNA structures. There are several alternative pathways of miRNA biogenesis that do not require components of the microprocessor complex. One of these pathways is biogenesis from mirtrons. Mirtrons are miRNAs that arise from the introns of the mRNA coding genes. These miRNAs are spliceosome-excised and are direct substrates for Dicer. However, there are also mirtrons that are not dependent on spliceosome. They are called splicing-independent-mirtron-like miRNAs (simtrons). Simtrons occur by a pathway that involves Drosha but does not require DGCR8 or Dicer [38].

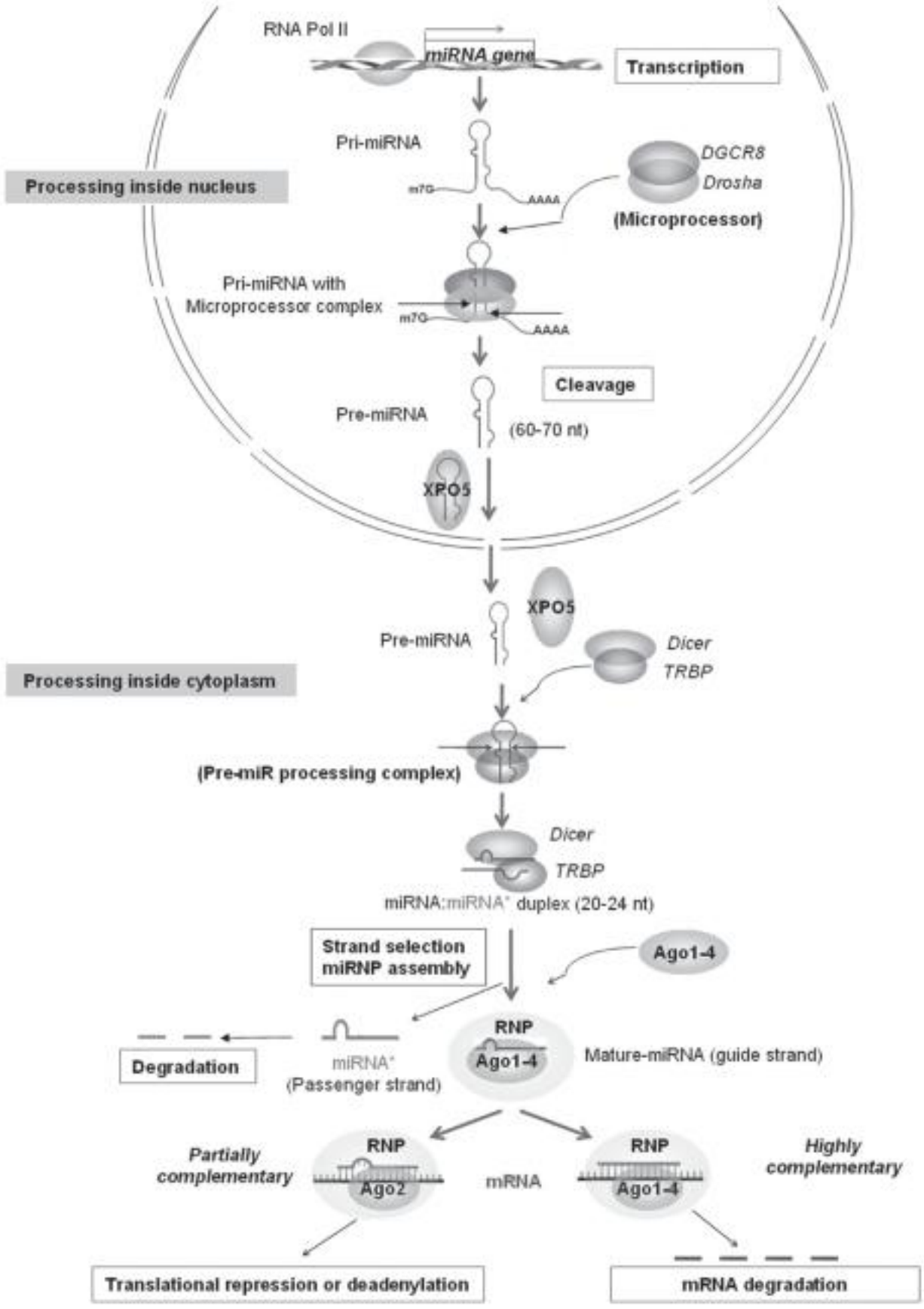

Figure 8: The canonical model of miRNA biogenesis [39].

1.3.2 MicroRNAs associated with EMT

EMT is regulated by EMT-TFs (Twist, Snail, ZEB1, ZEB2) at transcriptional level. Majority of these EMT-TFs is involved in transcriptional repression of E-cadherin. These EMT-TFs can be further regulated at post-trancriptional level by microRNAs. The most described microRNAs involved in EMT regulation are miRNAs that belong to miR-200 family, miR-205 and miR-192/215 [40,41].

MiR-200 family

MiR-200 family includes five members (miR-200a, miR-200b, miR-200c, miR-141 and miR-429) and it is divided into two clusters. First cluster is localised on chromosome 1 (miR-200a, miR-200b, miR-429) and the second cluster is localized on chromosome 12 (miR-200c, miR-141), (Figure 10). Since they are members of the same family, they have very similar seed sequences and thus they are targeting the same molecules. These miRNAs function as tumour suppressors and they are negative regulators of translation of ZEB1 and ZEB2. ZEB1 and ZEB2 are trancriptional repressors of E-cadherin and at the same time ZEB1 and ZEB2 negatively regulate expression of miR-200 family members. ZEB proteins and miR-200 family miRNAs t create together reciprocal regulation loops (Figure 9), [42]. Switching between EMT and MET is possible due to this ambiguous regulation. Expression levels of miR-200 family miRNAs are high in normal epithelia and significantly downregulated in carcinomas [43–45].

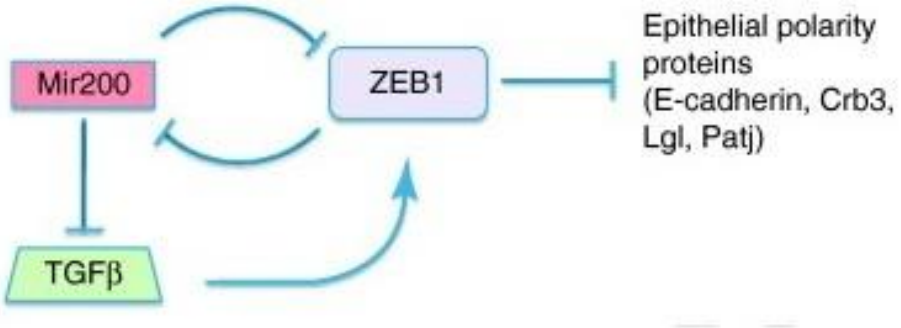

Figure 9: ZEB1 and miR-200 family regulation loop [46].

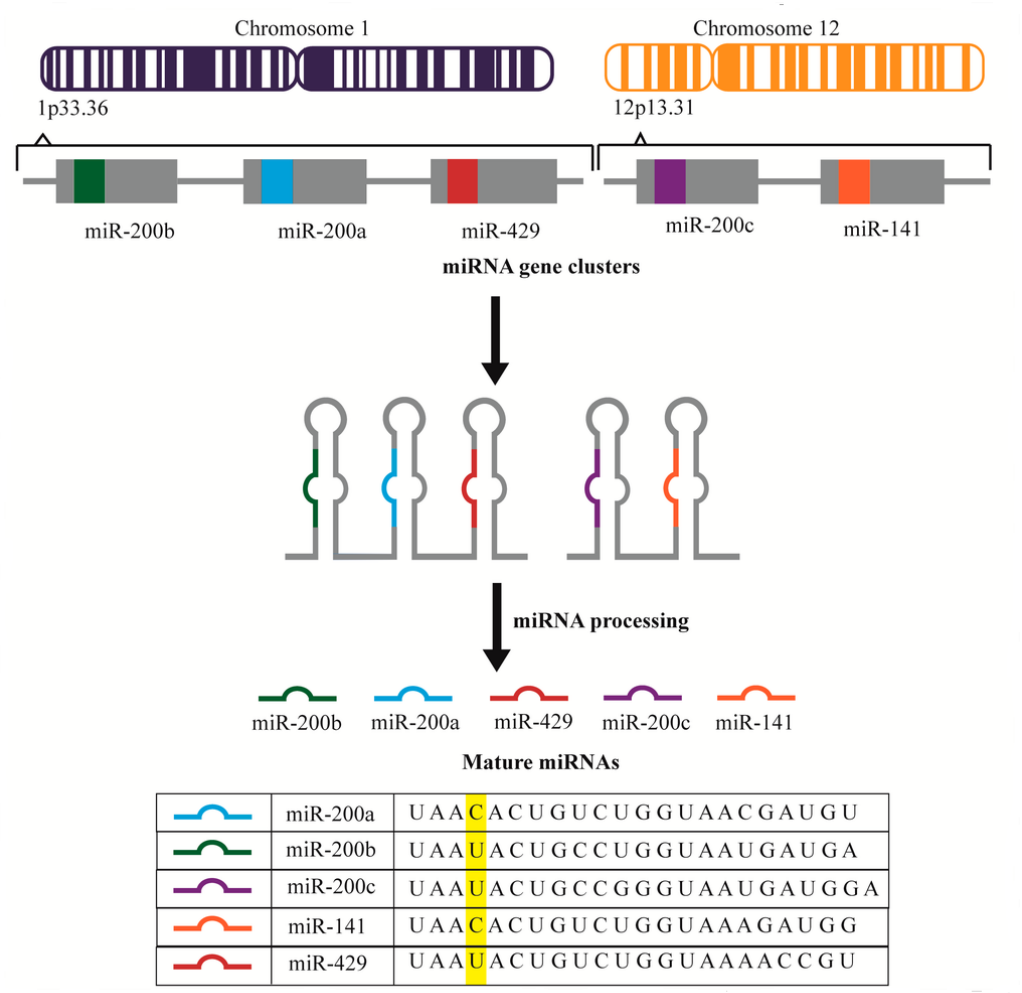

Figure 10: Sequences of miR-200 family [47].

MiR-205

MiR-205 is considered as an tumor oncosuppressor. This miRNA plays complex roles in carcinogenesis and tumor progression by acting either as a tumor suppressor or an oncogene depending on the tumor type. MiR-205 targets transcriptional repressor of E-cadherin ZEB1. However, promotion of EMT due to increased expression of this miRNA was observed in endometrial cancer cells. MiR-205 promoted EMT through targeting protein kinase B [48]. Dysregulation of miR-205 expression was found in various types of cancer including prostate, ovarian, nasopharyngeal, breast and urinary bladder [48–51].

MiR-192/215

MiR-192 and miR-215 are homologous miRNAs with functions in cell cycle, proliferation and repression of ZEB2. In contrary to repression of EMT by miR-200 family, repression of EMT by miR-192 and miR-215 does not rely on expression of ECM components [52]. In colorectal cancer cell lines is miR-192/215 associated with reduced cell proliferation [53]. Dysregulation of miR-192/215 is also linked to progressive renal glomerular and tubulointerstitial fibrosis [54].

2. Objectives

1) To validate the differences in expressions of E-cadherin and miR-429 in tissues of primary ccRCC and renal parenchyma tissues. Correlate the results with clinical-pathological data.

2) To evaluate TGFβ effects on E-cadherin expression, cell morphology and cell metabolic activity.

3) To evaluate capacity of miR-429 to reverse TGFβ effects.

4) To observe influence of miR-429 and TGFβ on cell migratory capacity.

3. Matherial and Methods

3.1 Chemicals

Absolute Ethanol (Lachema, Czech Republic)

Accutase (Gibco, USA)

McCoy's 5A medium (Sigma- Aldrich, USA)

Rosewell-Park Memorial Institute medium 1640 (RPMI1640) (Gibco, USA)

Minimum Essentials Medium (MEM) (Gibco, USA)

Opti-MEM Reduced Serum Media (Gibco, USA)

Dimethyl sulfoxide ≥99.5% (Sigma-Aldrich, USA)

Direct-zol mini prep kit (ZymoResearch, USA)

Qiazol Lysis Reagent (Qiagen, Germany)

Mitomycin C from Streptomyces caespitosus (Sigma-Aldrich Inc., Saint Louis, MO, USA)
GlutaMAX™ (Gibco, USA)

HyClone Sodium pyruvate (GE Healtcare Cell Culture, USA)

HyClone Penicilin/Streptomycin (GE Healtcare Cell Culture, USA)

HyClone Non-Essential Amino Acids (NEAA) (GE Healtcare Cell Culture, USA)

Dulbecco's phosphate buffered saline (PBS),(Sigma-Aldrich Inc., Saint Louis, MO, USA)

OPTI-MEM® Reduced Serum Medium 1× (Invitrogen, Carlsbad, CA, USA)

Trypan Blue Stain 0.4% (Invitrogen, Carlsbad, CA, USA)

Lipofectamine® RNAiMAX (Invitrogen, Carlsbad, CA, USA)

DEPC-Treated water (Ambion INC, Austin, Texas)

Acid Phenol: CHCl3 (Ambion INC, Austin, Texas)

MTT Formazan powder (Sigma-Aldrich Inc., Saint Louis, MO, USA)

mirVanaTM miRNA Isolation Kit (Ambion INC, Austin, Texas)

TaqMan® MicroRNA Reverse Transcription Kit, 1000 Reactions (Applied Biosystems, CA, USA)

TaqMan® High Capacity Reverse Transcription Kit, 1000 Reactions (Applied Biosystems, CA, USA)

TaqMan® MicroRNA Assays – hsa-miR-429 ,and RNU48 (Applied Biosystems, CA, USA), (Table I).

Table I: List of miRNA expression qPCR assays used in the study.

miRBase ID Release version 21	miRBase Accession No.	AB assay name	AB assay ID	Mature miRNA Sequence
hsa-miR-429	MIMAT0001536	hsa-miR-429	1024	UAAUACUGUCUGGUAAAACCGU
RNU48	NCBI Accession Number: NR_002745	RNU48	1006	GATGACCCCAGGTAACTCTGAGTGTGTCGCTGATGCCATCACCGCAGCGCTCTGACC

TaqMan® Assays – CDH1, CDH12, VIM, ZEB1, ZEB2 ,and PPIA (Applied Biosystems, CA, USA), (Table II).

Table II: List of gene expression qPCR assays used in the study.

Gene symbol	Entrez Gene ID	Gene name	Assay name	Assay ID
CDH1	999	cadherin 1, type 1, E-cadherin (epithelial)	CDH1	Hs01023894_m1
CDH12	1010	cadherin 12, type 2 (N-cadherin 2)	CDH12	Hs00362037_m1
VIM	7431	vimentin	VIM	Hs00958111_m1
ZEB1	6935	zinc finger E-box binding homeobox 1	ZEB1	Hs00232783_m1
ZEB2	9839	zinc finger E-box binding homeobox 2	ZEB2	Hs00207691_m1
PPIA	5478	peptidylprolyl isomerase A (cyclophilin A)	PPIA	Hs99999904_m1

Pre-miR™ miRNA Precursor Molecules – pre-miR-429 and pre-miR-Negative Control #1 (Ambion INC, Austin, Texas)

3.2 Instruments

Microcentrifuge 5424 (Eppendorf, Germany)

Thermal cycler T100 (Biorad, USA)

Quant Studio 12k flex (Applied Biosystems, USA)

FLUOstar Omega (BMG LABTECH, Germany)

Microscope CKX31, CKX41 (Olympus, Japan)

Camera DS126491 (Canon, Japan)

Nanodrop ND-1000 (Thermo Fisher Scientific, USA)

MagNA Lyser (Roche, Switzerland)

3.3 Patients

In this study expressions of miR-429 and E-cadherin were measured in 231 native frozen tissue samples (186 primary tumor tissues, 45 renal parenchyma tissues). Samples were divided into four groups - renal parenchyma (n=45), no progression (n=109), progression (n=29) and stage IV (n=48), (Table III). All patients underwent radical nephrectomy. Samples were obtained from Masaryk Memorial Cancer Institute in Brno, Czech Republic. All patients signed an informed consent form.

Table III: Characterization of patients involved in study

		Overall	Renal parenchyma	No progression	Progression	Stage IV
Number of patients		231	45	109	29	48
Age (years)	Range	31-86	39-80	31-86	42-84	34-81
	Median	63	61	64	63	64
Sex	Female	84	17	35	9	16
	Male	159	28	74	20	32

3.4 Tissue homogenization

For homogenization of samples was used mechanical homogenization by ceramic beads.

1. Add 500 µL of Lysis/Binding Buffer into the homogenization tube.
2. Place tissue into the homogenization tube with buffer. Keep on ice.
3. Place tube into MagnaLyzer and homogenise 2x for 60 sec at 6500 rpm.
4. Place the tube on ice.
5. Centrifuge for 5 min at 13400 rpm.
6. Replace supernatant into new microtube.
7. Immediatly perform RNA isolation.

3.5 RNA isolation from native frozen tissue

Total RNA enriched with small RNAs was isolated by commercial mirVana™ miRNA Isolation Kit. This kit combines extraction of nucleic acids by acidic phenol and RNA capture in glass fibre filter. RNA captured by filter is then washed and eluted.

1. Add 50 µL of miRNA Homogenate Additive to the supernatant. Incubate for 10 min on ice.
2. Add 500 µL of Acid-Phenol: Chloroform to the mixture.
3. Vortex for 15 sec.
4. Centrifuge for 5 min at 13 400 rpm.
5. Transfer aqueous phase into new tube.
6. Add 1.25 volumes of absolute ethanol. Mix by pipetting.
7. Place a filter cartridge into a collection tube.
8. Pipette 650 µL of ethanol/aqueous phase mixture onto the filter catridge.
9. Centrifuge for 30 sec at 13 400 rpm.
10. Discard filtrate from collection tube. Reuse collection tube.
11. Repeat steps 8. and 9. till whole volume of ethanol/aqueous phase mixture passes through the cartridge.
12. Pipet 700 µL of Wash Solution 1 onto the filter cartridge.
13. Centrifue for 30 sec at 13 400 rpm.

14. Remove filtrate form collection tube.
15. Pipette 500 µL of Wash Solution 2/3 onto the filter cartridge.
16. Centrifuge for 30 sec at 13 400 rpm.
17. Discard filtrate from collection tube.
18. Repeat steps 15. and 16. one more time.
19. Centrifuge empty cartridge for 1 min at 13 400 rpm.
20. Transfer the cartridge into new clean microtube.
21. Add 50 µL of Elution Solution (pre-heated to 95°C) onto the cartridge.
22. Centrifuge for 30 sec at 13 400 rpm
23. Discard the cartridge.
24. Measure concentration and purity of total RNA using NanoDrop® ND-1000
25. Store at -80°C.

3.6 RNA isolation from cell lines

For isolation of total RNA enriched with small RNAs from cell lines was chosen commercial kit Direct-zol RNA miniPrep. Lysis of cells was done by Qiazol reagent.

Lysis of cells

1. Discard media from well where cells are seeded.
2. Add 200 µL of Qiazol into the well.
3. Incubate for 5 min at room temperature.
4. Transfer the lysate into new microtube.

Isolation

1. Spin microtube with lysate for 5 min at 13 400 rpm.
2. Transfer supernatant into new clean microtube.
3. Add 200 µL of absolute ethanol. Mix by pipetting.
4. Pipette mixture onto the cartridge placed in collection tube.
5. Centrifuge for 1 min at 13 400 rpm.
6. Discard filtrate.

7. Pipette 400 µL of Direct-zol RNA pre Wash buffer onto the cartridge.
8. Centrifuge for 1 min at 13 400 rpm .
9. Discard filtrate.
10. Pipette 700 µL of RNA Wash Buffer onto the cartridge.
11. Centrifuge for 1 min at 13 400 rpm.
12. Discard filtrate.
13. Centrifuge empty cartridge for 2 min at 13 400 rpm.
14. Transfer cartridge to new clean microtube.
15. Pipette 30 µL of RNAse free water onto the cartridge.
16. Centrifuge for 1 min at 13 400 rpm.
17. Discard the cartridge.
18. Measure concentration and purity of total RNA using NanoDrop® ND-1000.
19. Store at -80°C.

3.7 MicroRNA specific reverse transcription

Since microRNAs are 18-25 nucleotides long there is a problem with use of conventional primers for reverse transcription. This problem is solved by use of microRNA specific stem loop primers. We used TaqMan® MicroRNA Reverse Transcription Kit.

1. In clean microtube prepare master mix according to table below (Table IV).

Table IV: Composition of miRNA RT master mix

Component	**Reagent volume [µL] per 10µL reaction**
100mM dNTPs (with dTTP)	0,10
MultiScribe Reverse Transcriptase, 50 U/ul	0,67
10x Reverse Transcription Buffer	1,00
Rnase Inhibitor, 20 U/uL	0,13
Nuclease-free watter	2,77
MiRNA specific primer	2,00
Total volume	**6,67**

2. Shortly wortex and keep on ice.

3. Dilute sample RNA to 6,67 ng/3,33 µL
4. Pipette 6,67 µL of RT master mix into strip well per reaction.
5. Add 3,33 µL of diluted RNA.
6. Shake the strip and then shortly spin down.
7. Incubate for 5 min on ice.
8. Set thermocycler according to table below (Table V).

Table V: Thermocycler conditions for RT.

Temperature [°C]	Time [min]
hold 16	30
hold 42	30
hold 85	5
hold 4	∞

9. Set reaction volume to 10 µL.
10. Run reverse transcription.
11. Store cDNA at -20°C.

3.8 Gene expression reverse transcription

Reverse transcription of mRNA was performed using High capacity cDNA reverse transcription kit. In contrary to miRNA specific reverse transcription this method uses pool of universal random primers.

1. In clean microtube prepare master mix according to the table below (Table VI).

Table VI: Composition of gene expression RT master mix.

Component	Reagent volume [µL] per 20µL reaction
100mM dNTPs (with dTTP)	0,80
MultiScribe Reverse Transcriptase, 50 U/ul	1,00
10x Reverse Transcription Buffer	2,00
10x Reverse Transcription random primers	2,00
Nuclease-free watter	4,20
Total volume	**10,00**

2. Shortly vortex. Keep on ice.

3. Dilute sample RNA to 400 ng/10 µL for RNA from cell lines and to 750 ng/10 µL for RNA from native frozen tissue.
4. Pipet 10 µL of master mix per reaction.
5. Add 10 µL of diluted RNA.
6. Shake the strip and spin down.
7. Incubate for 5 min on ice.
8. Set cycler according to table below (Table VII).

Table VII: Thermocycler conditions for RT

Temperature [°C]	Time [min]
hold 25	10
hold 37	120
hold 85	5
hold 4	∞

9. Set reaction volume to 20 µL.
10. Run reverse transcription
11. Store cDNA at -20°C.

3.9 Quantitative real time polymerase chain reaction

Relative gene/miRNA expression was measured by quantitative real time polymerase chain reaction (qRT-PCR). We used hydrolysis TaqMan™ assays. Analysis was done on qRT-PCR instrument Quant studio 12k flex. Measurment was performed in duplicates for each sample.

<u>microRNA expression</u>

1. Prepare master mix according to the table on next page (Table VIII).

Table VIII: Composition of miRNA qRT-PCR master mix

Component	Reagent volume [µL] per 15µL reaction
Universal no UNG Master Mix	7,50
Nuclease-free water	5,75
Probe	0,75
Total volume	14,00

2. Prepare 384 well optical reaction plate.
3. Pipette 14 µL of master mix per sample into a well.
4. Add 1 µL of cDNA to the well.
5. Pipette 1 µL of Nucleas-free water into two wells as non-template control.
6. Place adhesive optical foil onto the reaction plate.
7. Centrifuge the well plate for 1 min at 900 rpm.
8. Set cycler according to the table below (Table IX).

Table IX: Thermocycler conditions for miRNA qRT-PCR

Temperature [°C]	Time [s]	Cycles
50	120	hold
95	600	hold
95	15	45
65	60	

9. Set reaction volume to 15 µL.
10. Place the plate into the cycler.
11. Start run.
12. Analyze the results using Applied Biosystems software.
13.

Gene Expression

1. Prepare master mix according to the table on next page (Table X).

Table X: Composition of gene expression master mix

Component	Reagent volume [µL] per 15µL reaction
TaqMan Gene Expression Master Mix	7,50
Nuclease-free water	5,75
Probe	0,75
Total volume	14,00

2. Prepare 384 well optical reaction plate
3. Pipette 14 µL of master mix per sample into a well.
4. Add 1 µL of cDNA to the well.
5. Pipette 1 µL of Nucleas-free water into two wells as non-template control.
6. Place adhesive optical foil onto the reaction plate.
7. Centrifuge the well plate for 1 min at 900 rpm.
8. Set the cycler according to the table below (Table XI).

Table XI: Thermocycler conditions for gene expression qRT-PCR

Temperature [°C]	Time [s]	Cycles
50	120	hold
95	600	hod
95	15	45
65	60	

9. Set reaction volume to 15 µL.
10. Place the plate into the cycler.
11. Start run.
12. Analyze the results using Applied Biosystems software.

3.10 Analysis of the expression data

For analysis of expression data, $2^{-\Delta Ct}$ method was used. MiRNA expression was normalized to RNU48 and gene expression data to PPIA.

$$\Delta CT(\text{target gene}) = Ct(\text{target gene}) - Ct(\text{endogenous control})$$

$$RQ^*(\text{target gene}) = 2^{-\Delta Ct}(\text{target gene})$$

*Relative quantity

3.11 *In vitro* functional analyses

For *in vitro* analyses were chosen three ccRCC cell lines. Cell lines were obained from ATCC and cultivated in recommended media.

3.11.1 Cell lines

ACHN

- Derived from metastatic site (malignant pleural effusion) of renal cell adenocarcinoma, male, caucasian, 22 years old.
- Cultivated in Minimum Essential Medium (MEM) supplemented with 10% fetal bovine serum (FBS), 1% non-essential amino acids (NEAA), 1% sodium pyruvate, 1% GlutaMAX, 100 µg/ ml Streptomycin and 100 U/ml penicilin. Cells were cultivated under these conditions - temperature 37°C, 95% humidity and atmosphere with 5% CO_2.

Caki-2

- Derived from primary clear cell renal cell carcinoma, male, caucasian, 69 years old.
- Cultivated in McCoy's 5A medium supplemented with 10% FBS, 1% GlutaMAX, 100 µg/ ml Streptomycin and 100 U/ml penicilin. Cells were cultivated under these conditions - temperature 37°C, 95% humidity and atmosphere with 5% CO_2.

786-0

- Derived from primary renal cell adenocarcinoma, male, caucasian, 58 years old.
- Cultivated in Roswell Park Memorial Institute (RPMI) 1640 medium supplemented with 10% FBS, 1% GlutaMAX, 1% sodium pyruvate, 100 µg/ml Streptomycin and 100

U/ml penicilin. Cells were cultivated under these conditions - temperature 37°C, 95% humidity and atmosphere with 5% CO_2.

3.11.2 EMT induction

In this study we induced EMT using transforming growth factor β (TGFβ). One day after the cells were seeded, standard medium was changed to a medium with addition of TGFβ. Used concentration of TGFβ was 10 ng/µl. Effects of TGFβ were observed after two and four days after addition of TGFβ.

3.11.3 Transfection

Method of transient transfection was used for artificial overexpression of miR-429 in RCC cell lines. During transient transfection nucleic acids exist in cells only for limited time. Depending on the construct used, generally transiently expressed transgene can be detected from 1 to 7 days. Transiently transfected cells are typically harvested from 24 to 96 hours after transfection. The RCC cells were transfected by oligonucleotides pre-miR-429 and pre-miR negative control #1. As a transfecting reagent we used Lipofectamine RNAiMax. Concentration of oligonucleotides used in experiments was 33,3 nM per well (24 well plate). Amounts of reagents were multiplied by 5 for experiments performed in 6 well plates.

<u>Cell seeding</u>

1. Prepare 24 well plate.
2. Seed cells in concentration - $30*10^4$ cells/well (Caki-2), $25*10^4$ cells/well (ACHN), and $20*10^4$ cells/well (786-0). Use complete relevant medium without antibiotics.
3. Leave the cells in incubator for 24 h.

<u>Transfection</u>

1. Prepare two clean microtubes.
2. Pipette 50 µL of opti-MEM medium into each tube.

3. Add 4 µL of oligonucleotide (5 pmol/µl) to the one tube.
4. Add 1 µL of Lipofectamine RNAiMAX to the another one.
5. Incubate for 5 min at room temperature.
6. Pipette the content of tube with oligonucleotide into the tube with lipofectamine.
7. Incubate for 20 min.
8. Pipette 100 µL of mixture into the well with cells.
9. Put the plate with cells into the incubator.

3.11.4 MTT assay

This method is based on conversion of soluble MTT dye (3-(4,5-dimethylthiazol-2-yl)-2,5-diphenyltetrazolium bromide) to insoluble formazan. Conversion can be done only by living cells. The exact cellular mechanism of MTT reduction into formazan is not well understood, but likely involves reaction with NADH or similar reducing molecules that transfer electrons to MTT. The quantity of produced formazan is measured photometrically. Changes in absorbance reflect the metabolic activity of cells. Strenght of the signal is dependent on several factors including metabolic activity of cells, number of cells in well and incubation time. Absorbance maximum of formazan is at 570 nm.

1. Pipette 50 µL of MTT solution into a well (24 well plate) where cells are seeded.
2. Shake the plate and put it into the incubator.
3. Incubate for 2 hours.
4. Discard medium.
5. Add 500 µL of DMSO into the well.
6. Shake the plate.
7. Measure absorbance at 570 nm using FLUOstar Omega photometer.

3.11.5 Scratch wound assay

Scratch wound assay is a method for *in vitro* evaluation of cell migratory capacity. Method is based on creating a "scratch" into the cell monolayer and wound is then observed in time. Scratch wound assay is usually performed on 6 well plates. We compared differences in cell free area after 12 h (Caki-2, 786-0) and after 24 h (ACHN).

1. Seed cells on 6 well plate in following concentrations, $30*10^4$ cells/well (ACHN, Caki-2) and $20*10^4$ cells/well (786-0).
2. Cultivate for 24 h.
3. Add 50 µL of mitomycin (0,5 mg/ml) into the well.
4. Place the plate into the incubator.
5. Incubate for 1 hour.
6. Use a 1000 µL pipette tip for creating a scratch into the cell monolayer.
7. Discard the medium.
8. Rinse the cells with 2 ml of PBS.
9. Discard the PBS.
10. Pipette 2,5 ml of medium.
11. Take a picture of the scratch area at 0h, 12h and 24h.
12. Analyze the data using TS scratch software.

3.12 Statistical evaluation

Statistical analysis of the data was performed using GraphPad Prism 5 software. For validation phase of study was used Kruskal-Wallis one-way analysis of variance, Mann-Whitney non parametric test, ROC analysis and Kaplan-Meier survival analysis. *In vitro* experiments were evaluated by a two-tailed non-parametric t-test. P values lower than 0.05 were considered as statistically significant.

4. Results

4.1 Expression of miR-429 in patient samples

Based on previous data measured in our laboratory we decided to validate miR-429 in independent 231 ccRCC samples. Samples in this validation cohort included 186 primary tumor tissues and 45 renal parenchyma tissues. MiR-429 expression was significantly downregulated in primary tumor tissues in comparison to renal parenchyma ($p<0.0001$), (Figure 11). Tumor tissue samples were further divided into three subgroups (no progression, progression, stage IV). We found out that miR-429 was significantly downregulated in primary tumor tissues of stage IV patients when compared to primary tumor tissues of patients without progression ($p<0.0001$) and primary tumor tissues of patients with progression ($p=0.0115$), (Figure 12). Further, we evaluated influence of miR-429 expression levels on disease-free survival (DFS) of ccRCC patients. Patients with higher expression levels of miR-429 showed significantly longer time to recurrence of ccRCC after radical nephrectomy than patients with lower expression levels of miR-429 ($p=0.0105$), (Figure 13). As endogenous control was used RNU48.

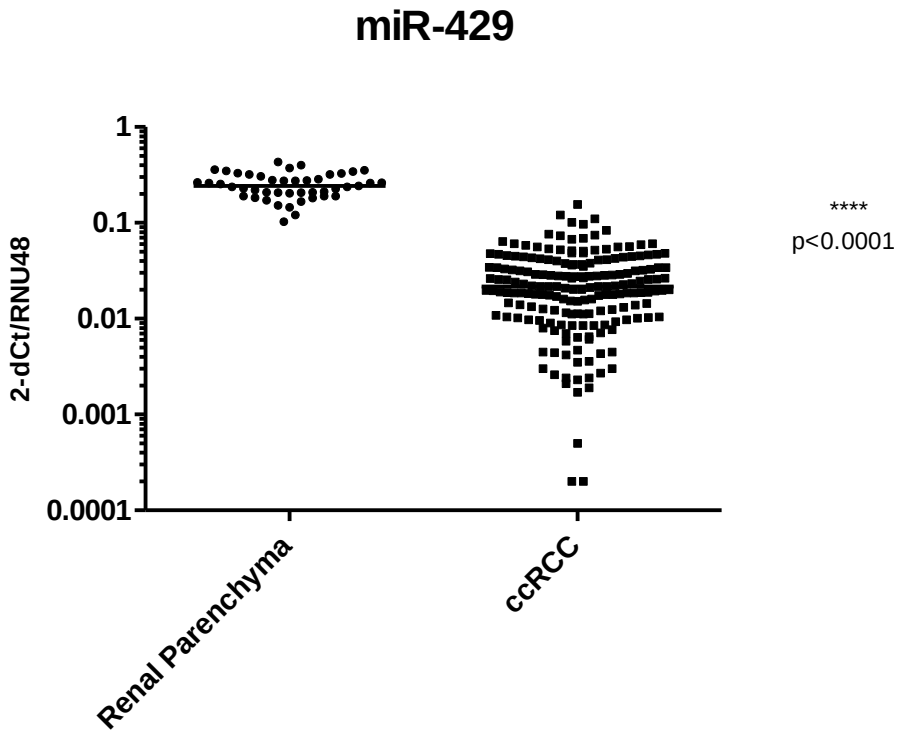

Figure 11: Expression of miR-429 in renal parenchyma vs. ccRCC.

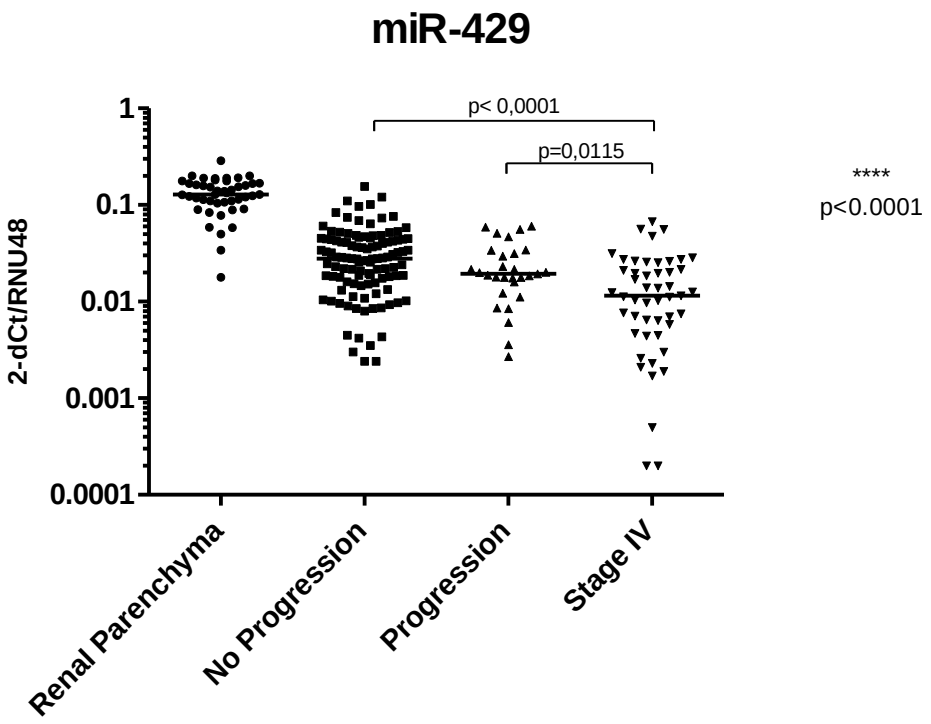

Figure 12: Expression of miR-429 in renal parenchyma and ccRCC samples. RCC samples were divided into three subgroups (no progression, progression, stage IV).

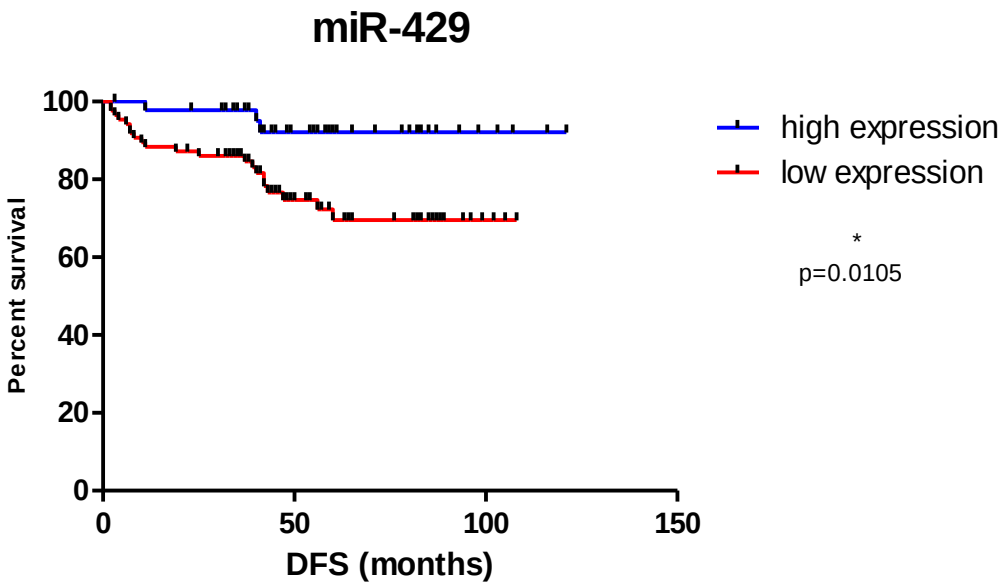

Figure 13: Kaplan-Meier survival analysis. Patients with higher miR-429 expression vs. patients with lower miR-429 expression in primary tumor tissue.

4.2 E-cadherin expression in patient samples

E-cadherin is the most well-known EMT marker. We measured expression of E-cadherin in 231 ccRCC samples. Cohort included 186 primary tumor tissues and 45 renal parenchyma tissues. E-cadherin expression was significantly downregulated in primary tumor tissues in comparison to renal parenchyma tissues ($p<0.0001$), (Figure 14). Tumor tissue samples were further divided into three subgroups (no proression, progression, stage IV). We found out that E-cadherin was significantly downregulated in primary tumor tissues of stage IV patients when compared to primary tumor tissues of patients without progression ($p<0.0001$) and primary tumor tissues of patients with progression ($p=0.0100$), (Figure 15). Further, we evaluated influence of E-cadherin expression levels on DFS of ccRCC patients. Patients with higher expression levels of E-cadherin did not showed any significant differences in DFS when compared to patients with lower expression levels of E-cadherin (Figure 16).

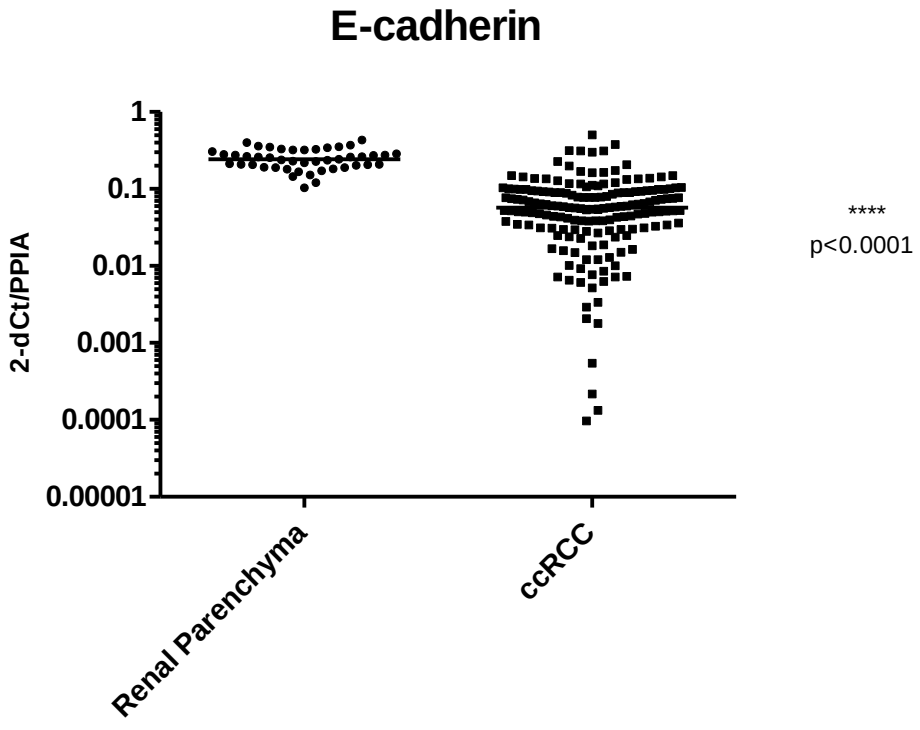

Figure 14: Expression of E-cadherin in renal parenchyma vs. ccRCC.

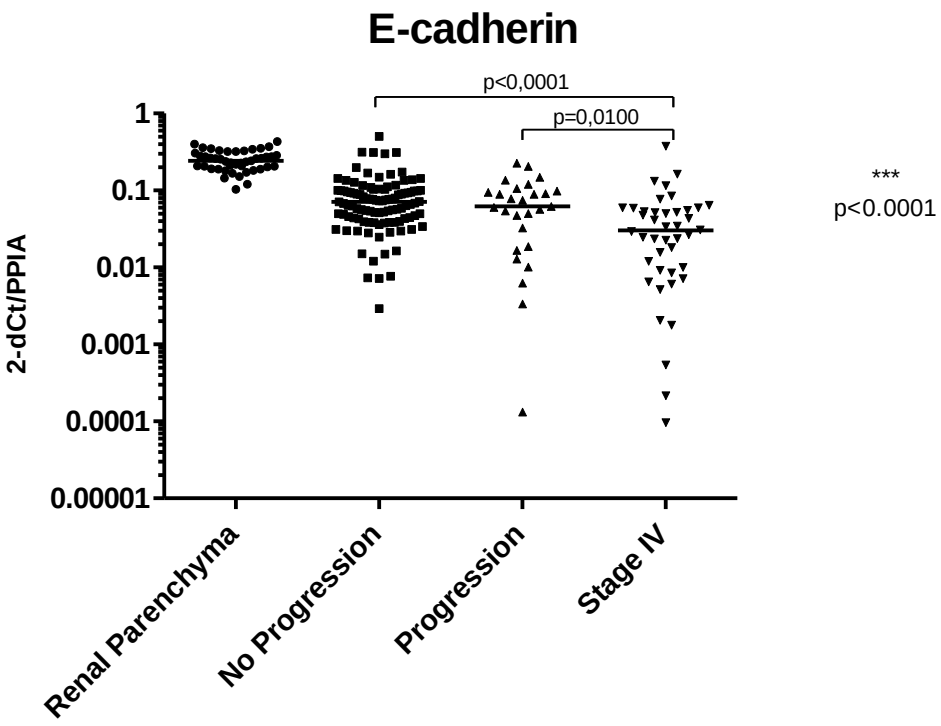

Figure 15 : Expression of E-cadherin in renal parenchyma and ccRCC samples. RCC samples were divided into three subgroups (no progression, progression, stage IV). As endogenous control was used PPIA.

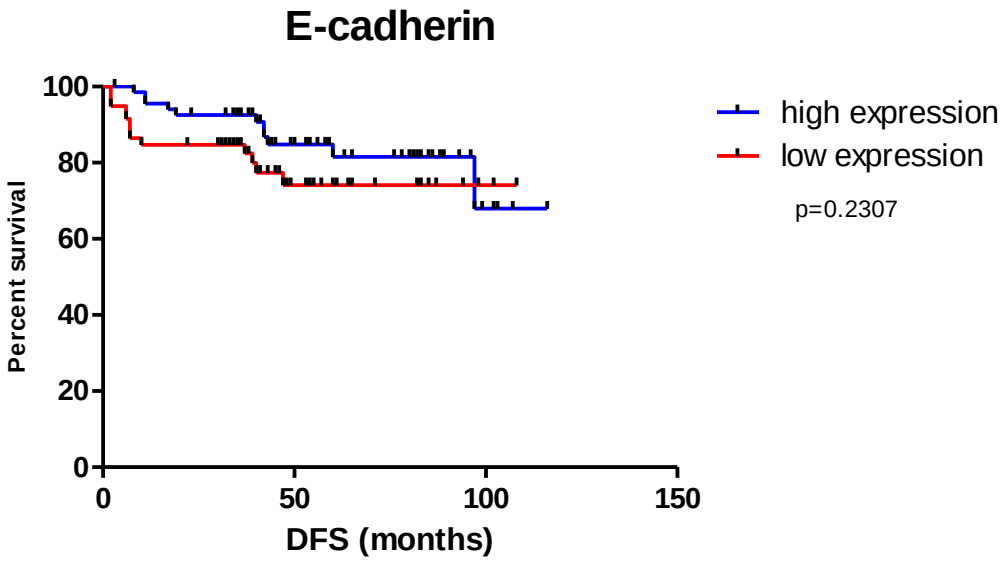

Figure 16: Kaplan-Meier survival analysis. Patients with high E-cadherin expression vs. patients with low E-cadherin expression in primary tumor tissue.

4.3 Effects of TGFβ on RCC cell lines

Three RCC cell lines (ACHN, Caki-2, 786-0) were treated with 10ng/ml TGFβ. Cytokine was added into the media one day after seeding of cells.

4.3.1 Effects of TGFβ on E-cadherin expression

ACHN and Caki-2 cell lines did not show any significant differences in E-cadherin expression between cells treated with TGFβ and control cells (MOCK). However, trend in E-cadherin downregulation was observed in TGFβ treated cells in cell lines-ACHN (Figure 17, Figure 18) and Caki-2 (Figure 19, Figure 20) for both day 2 and day 4 after the TGFβ treatment. Cell line 786-0 showed significant downregulation of E-cadherin expression in cells treated with TGFβ when compared to control cells both on day 2 ($p=0.0054$) and day 4 ($p=0.0053$), (Figure 21, Figure 22). As endogenous control was used PPIA. Presented data are from three independent biological replicates.

ACHN

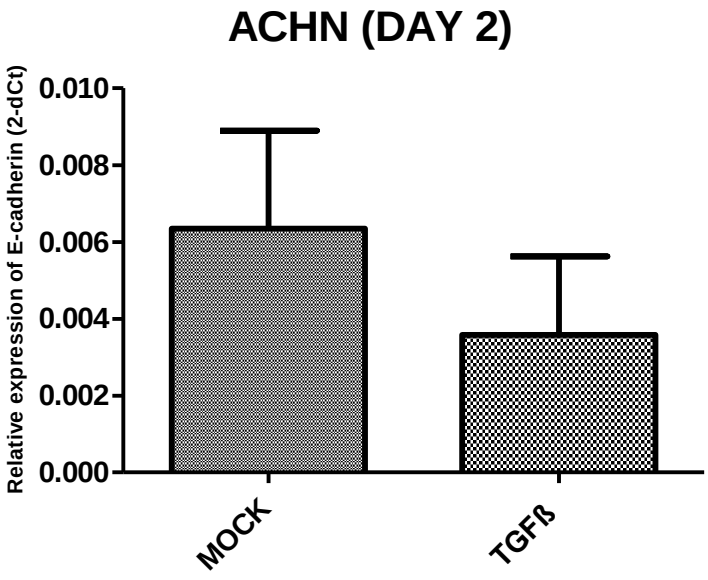

Figure 17: E-cadherin expression in ACHN cells treated with TGFβ vs. MOCK. Day 2.

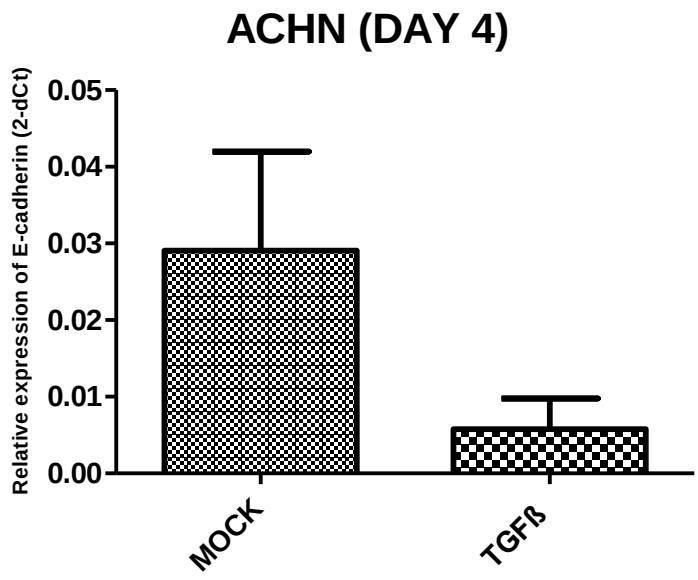

Figure 18: E-cadherin expression in ACHN cells treated with TGFβ vs. MOCK. Day 4.

Caki-2

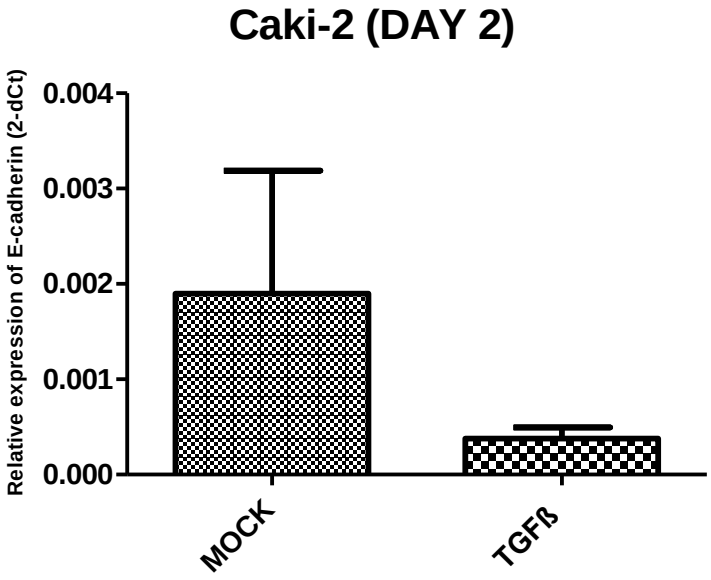

Figure 19: E-cadherin expression in Caki-2 cells treated with TGFβ vs. MOCK. Day 2.

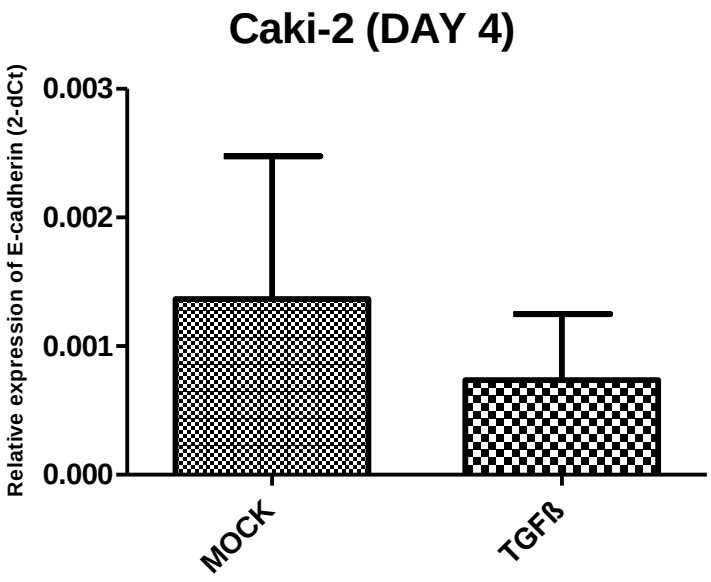

Figure 20: E-cadherin expression in Caki-2 cells treated with TGFβ vs. MOCK. Day 4.

<u>786-0</u>

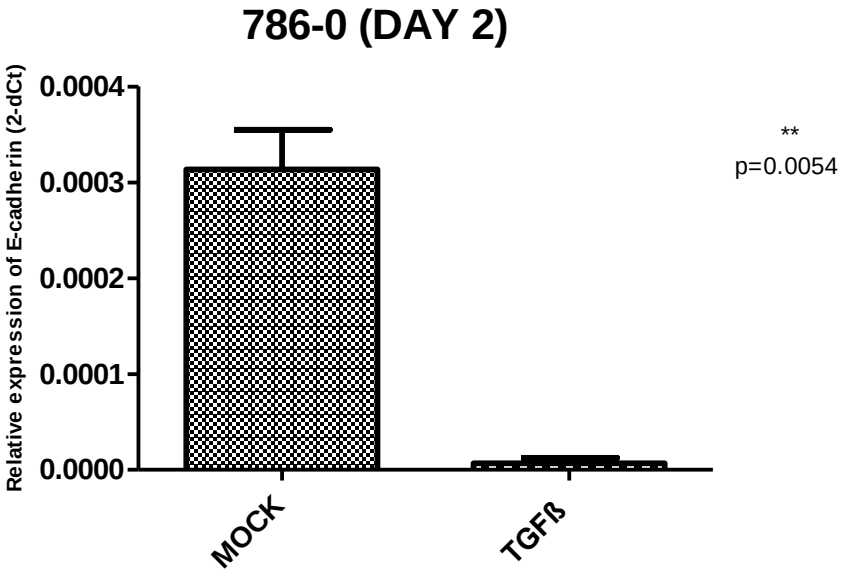

Figure 21: E-cadherin expression in 786-0 cells treated with TGFβ vs. MOCK. Day 2.

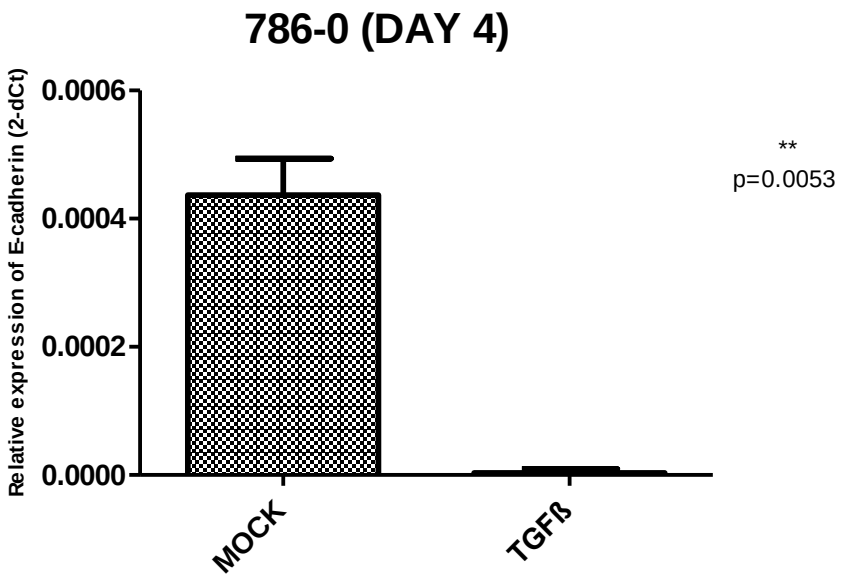

Figure 22: E-cadherin expression in 786-0 cells treated with TGFβ vs. MOCK. Day 4.

4.3.2 Effects of TGFβ on expression of other EMT-related genes and miR-429 in 786-0 cell line

Since the decreasing trend in E-cadherin expression after TGFβ treatment was significant only in 786-0 cell line, we decided to measure expression of other EMT-related genes (N-cadherin, vimentin, ZEB1, ZEB2) and miR-429 in this cell line. Cells were treated with 10 ng/ml TGFβ and expressions of genes and miR-429 were measured 2 days after the treatment. Any of the measured genes did not show significant differences in expression between cells treated with TGFβ and control cells (MOCK), (Figure 23). N-cadherin expression was not present at all. As endogenous controls were used RNU48 for miRNA expression and PPIA for gene expression. Presented data are from three independent biological replicates.

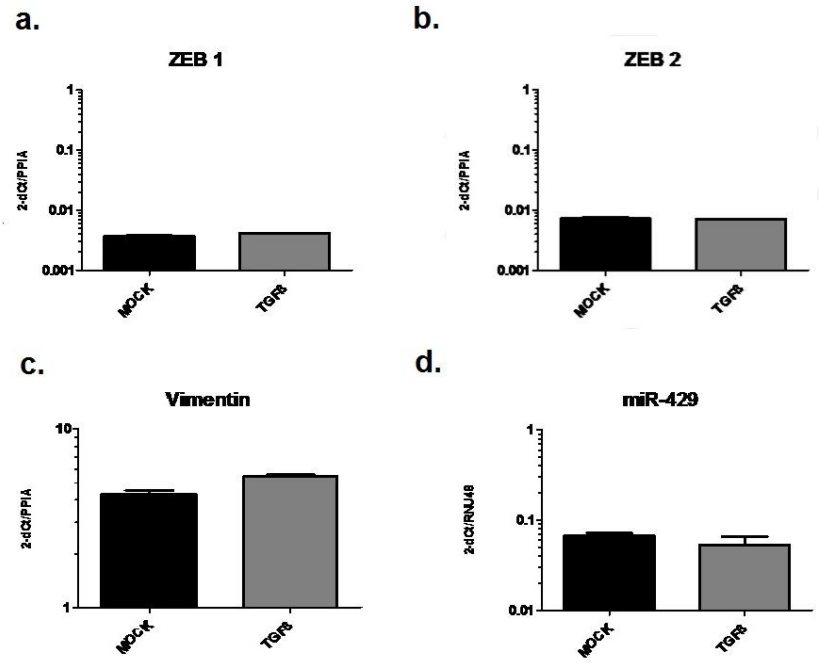

Figure 23: Expression of EMT-related genes and miR-429 in 786-0 cell line treated with TGFβ and 786-0 control cells (a. ZEB1, b. ZEB2, c. Vimentin, d. miR-429).

4.3.3 Effects of TGFβ on cell morphology

ACHN, Caki-2, and 786-0 cell lines were treated with 10 ng/ml TGFβ. Images (100x magnified) of the cells were taken 2 and 4 days after the addition of TGFβ into the media. Ideally, cells treated with TGFβ should change their shape from cuboidal to spindle-shaped. Since evaluation by observation is highly subjective method, it can not be said that any of the cell lines showed significant differences in morphology between cells treated with TGFβ and control cells (MOCK). Subjectively were observed slight changes in ACHN morphology (Figure 24), no changes in Caki-2 morphology (Figure 25), and the biggest change in morphology was observed in 786-0 cell line (Figure 26).

ACHN

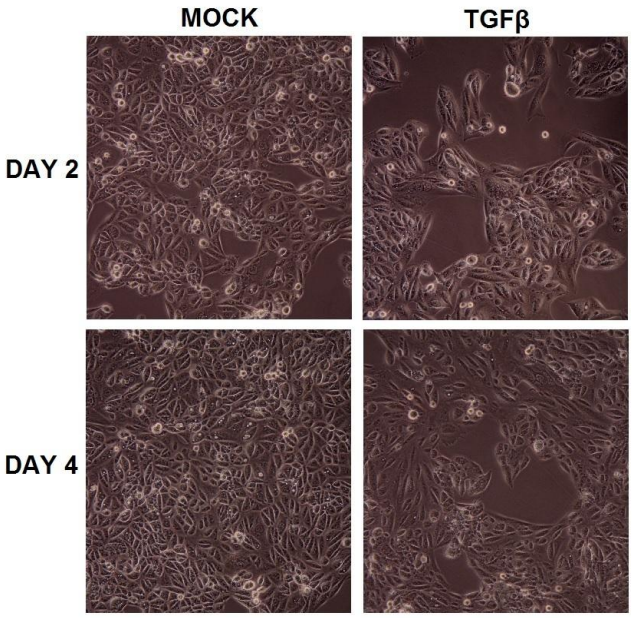

Figure 24: Images of ACHN cell line without and with TGFβ treatment. TGFβ treated cells appear slighty longer than the controls.

Caki-2

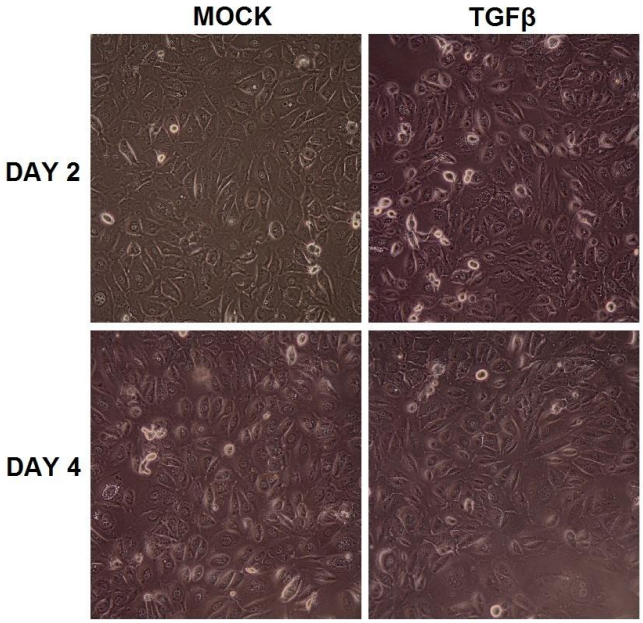

Figure 25: Images of Caki-2 cell line. No change in morphology was observed.

786-0

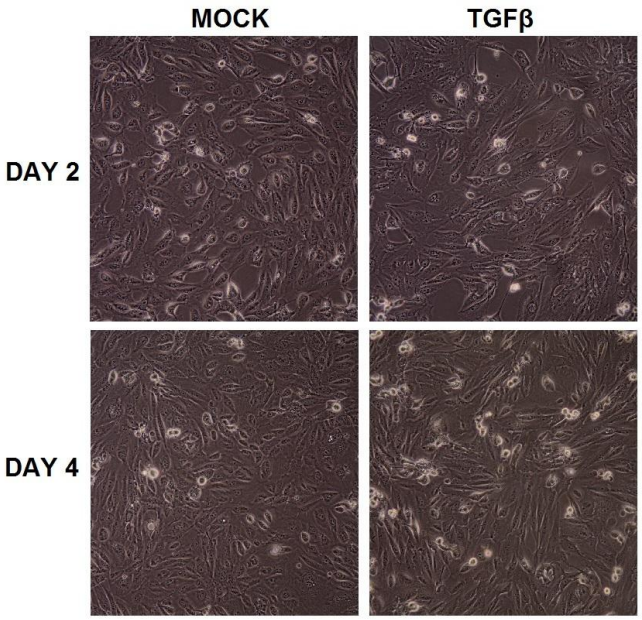

Figure 26: Images of 786-0 cell line without and with TGFβ treatment. TGFβ treated cells appear more spindle-shaped than the controls.

4.3.4 Effects of TGFβ on metabolic activity of cells

Metabolic activity of cells was measured by MTT test. TGFβ was added into the media one day after seeding. Incubation time with MTT was 2 hours and absorbance was measured for three days. MTT test was done in three technical replicates and in three independent biological replicates. No difference in metabolic activity was observed in cells treated with TGFβ in comparison to control cells (NC, MOCK) in all three cell lines- ACHN (Figure 27), Caki-2 (Figure 28) and 786-0 (Figure 29). TGFβ does not have any significant influence on metabolic activity of RCC cell lines ACHN, Caki-2 and 786-0.

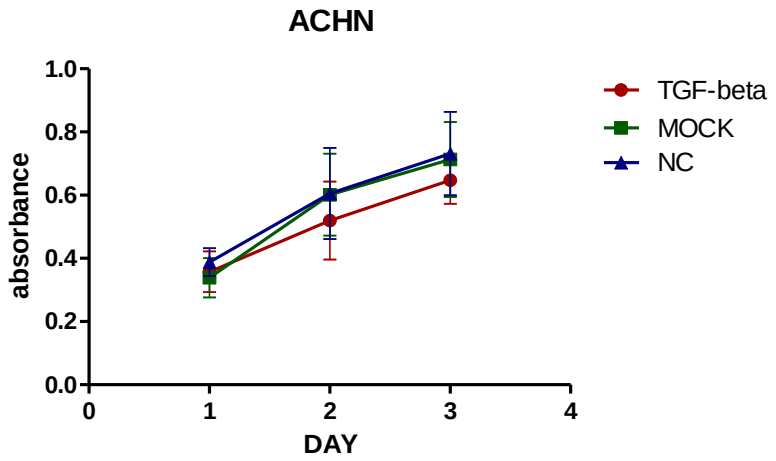

Figure 27: MTT test of ACHN cell line. Cells treated with TGFβ vs. MOCK vs. NC.

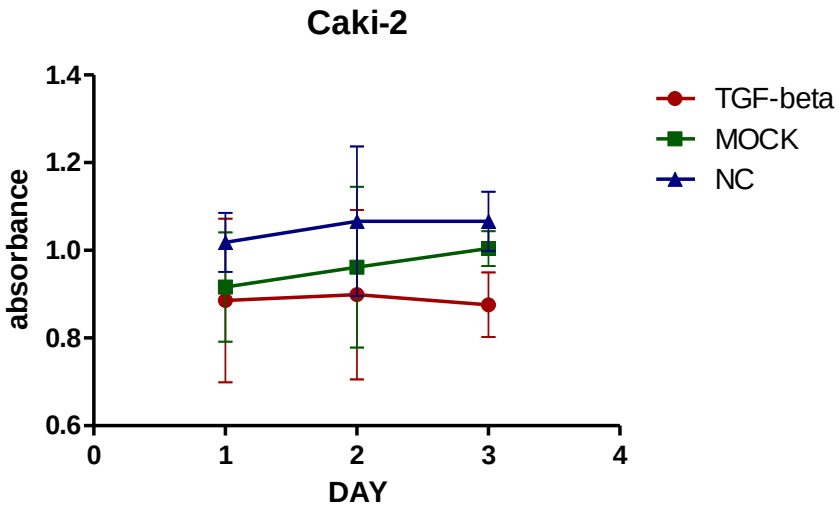

Figure 28: MTT test of Caki-2 cell line. Cells treated with TGFβ vs. MOCK vs. NC.

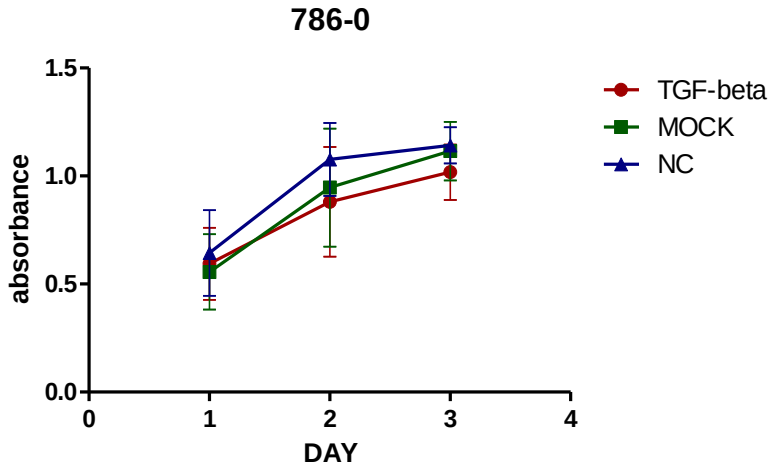

Figure 29: MTT test of 786-0 cell line. Cells treated with TGFβ vs. MOCK vs. NC.

4.4 Effects of miR-429 and TGFβ on E-cadherin expression levels

Cells were transfected with 33 nM of pre-miR-429 and negative control #1 (MOCK) and treated with 10 ng/ml of TGFβ one day after seeding. Expression levels of E-cadherin were measured 2 and 4 days after transfection and treatment. Any significant differences in E-cadherin expression between cells transfected with pre-miR-429 + treated with TGFβ and cells treated with TGFβ were not present in ACHN cells (Figure 30, Figure 31), Caki-2 cells (Figure 32, Figure 33) and 786-0 cells(Figure 34, Figure 35). Decresing trend in E-cadherin expression was observed in all three cell lines after TGFβ treatment, on the other hand cells transfected with pre-miR-429 + treated with TGFβ had very similar expression of E-cadherin as control cells. MiR-429 has probably capacity to restore E-cadherin expression in TGFβ treated RCC cells. Presented data are from three independent biological replicates. As endogenous control was used PPIA.

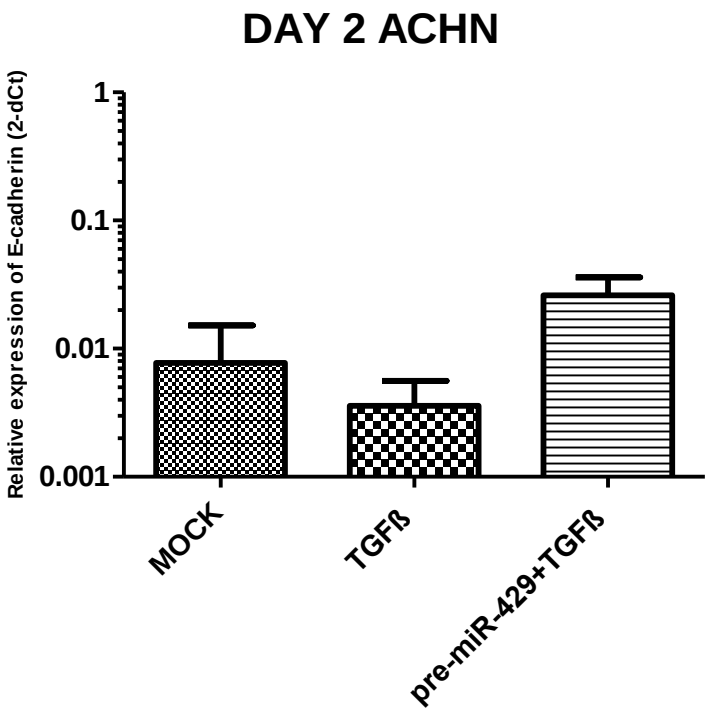

Figure 30: E-cadherin expression in ACHN cells treated with TGFβ and cells transfected with pre-miR-429 + treated with TGFβ. Day 2.

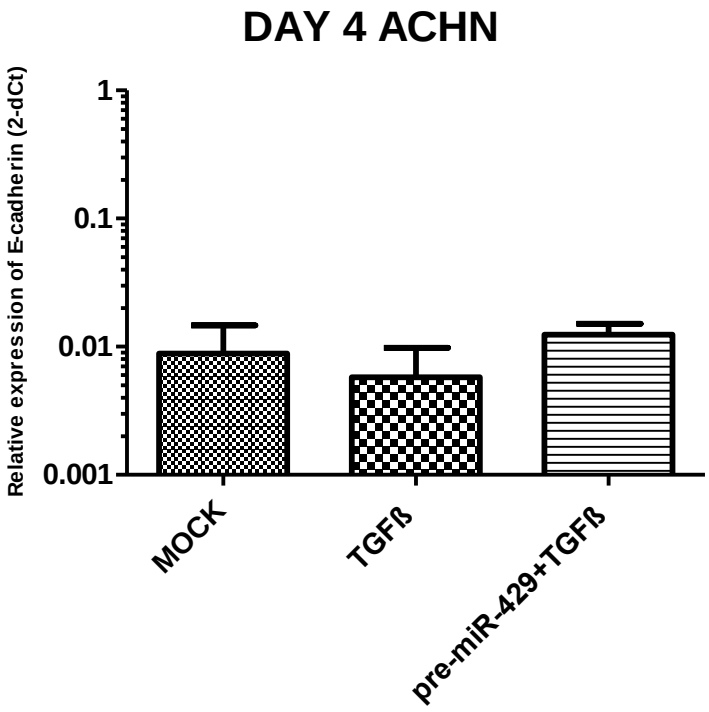

Figure 31: E-cadherin expression in ACHN cells treated with TGFβ and cells transfected with pre-miR-429 + treated with TGFβ. Day 4.

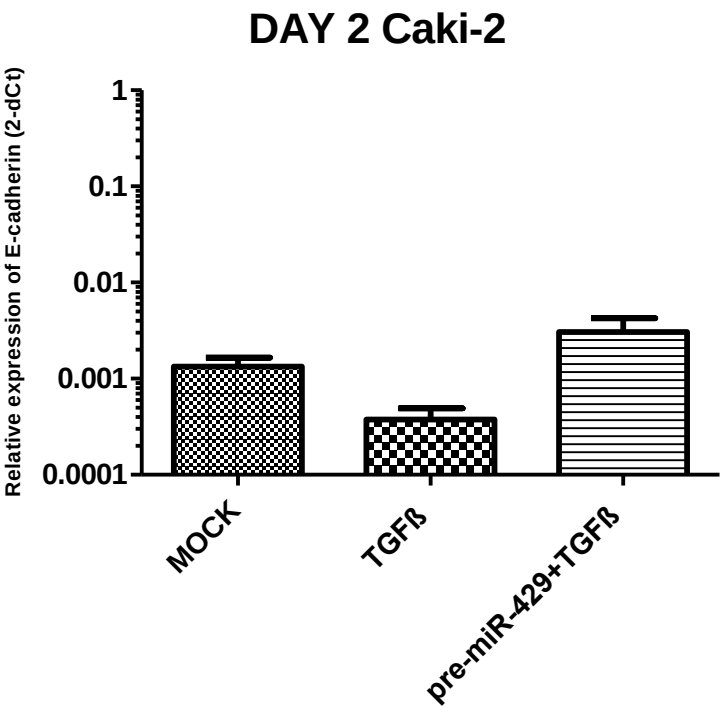

Figure 32: E-cadherin expression in Caki-2 cells treated with TGFβ and cells transfected with pre-miR-429 + treated with TGFβ. Day 2.

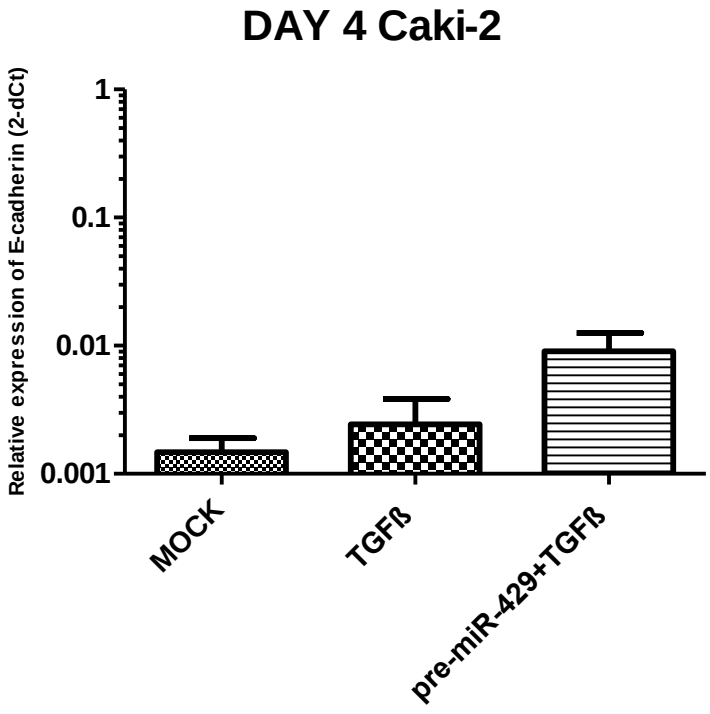

Figure 33: E-cadherin expression in Caki-2 cells treated with TGFβ and cells transfected with pre-miR-429 + treated with TGFβ. Day 4.

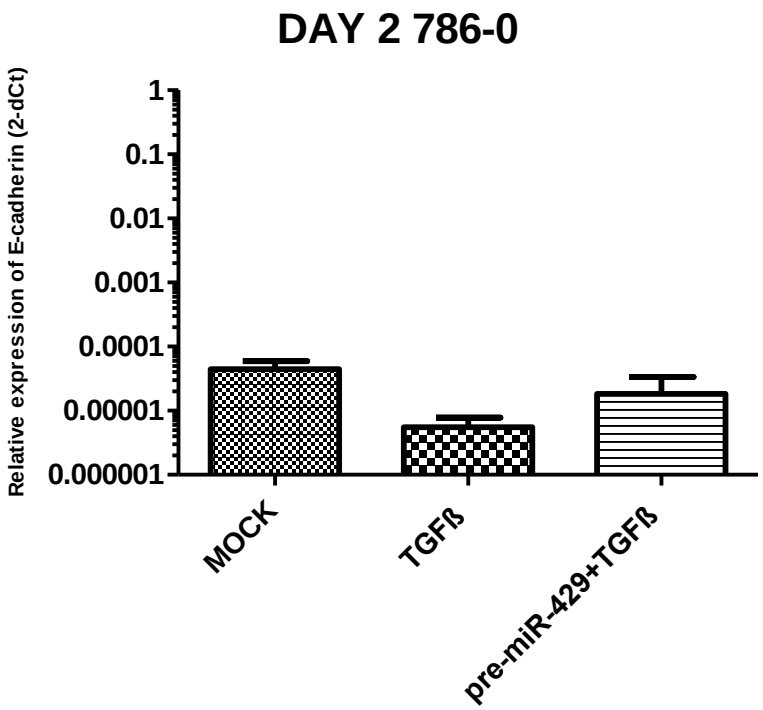

Figure 34: E-cadherin expression in 786-0 cells treated with TGFβ and cells transfected with pre-miR-429 + treated with TGFβ. Day 2.

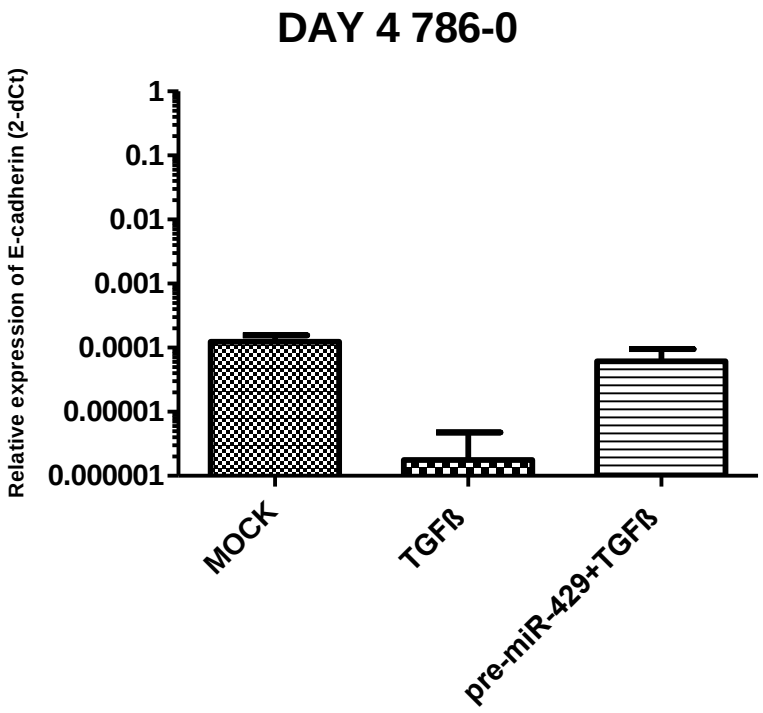

Figure 35: E-cadherin expression in 786-0 cells treated with TGFβ and cells transfected with pre-miR-429, transfected with pre-miR-429 + treated with TGFβ. Day 4.

4.5 Effects of miR-429 and TGFβ on cell migratory capacity

Migratory capacity was measured by scratch wound assay. Cells were transfected with negative control #1 (MOCK), pre-miR-429 and treated with TGFβ one day after seeding. One day after transfection and treatment the scratch was made. Images (40x magnified) were taken after 12 h (Caki-2, 786-0) and 24 h (ACHN). ACHN cell line did not show any differences in relative cell migration independently on transfection and treatment (Figure 36, Figure 37). Caki-2 cell line did not show any differences in relative cell migration between transfected/treated cells and control cells as well (Figure 38, Figure 39). 786-0 cell line showed significantly increased relative cell migration of cells treated with TGFβ in comparison to control cells ($p=0.0011$) and cells transfected with pre-miR-429 + treated with TGFβ ($p<0.0001$). This observation proves ability of miR-429 to reverse effects of TGFβ on cell migration in 786-0 cell line (Figure 40, Figure 41). Presented data are from three independent biological replicates.

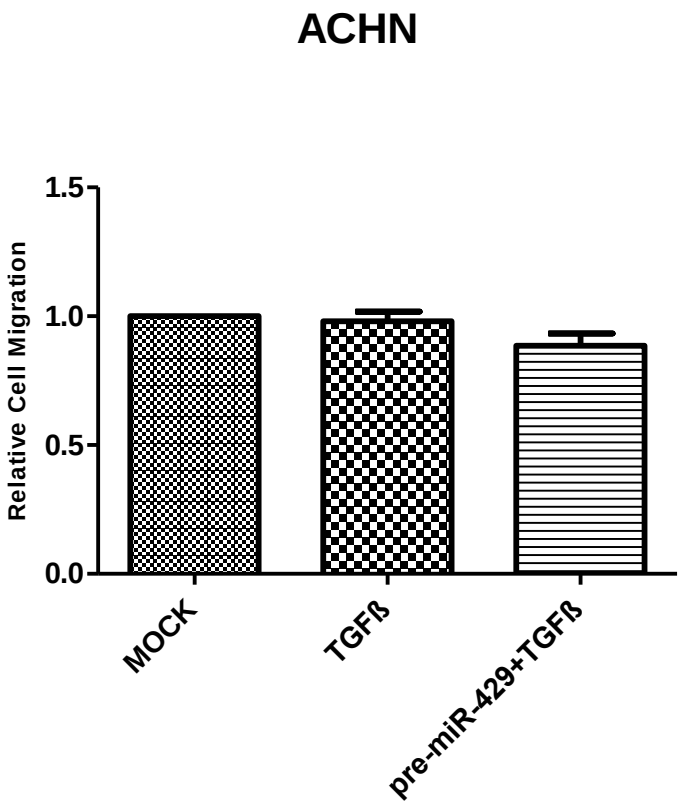

Figure 36: Relative cell migration of ACHN cells transfected with negative control #1 (MOCK), cells treated with TGFβ and cells transfected with pre-miR-429 + treated with TGF β.

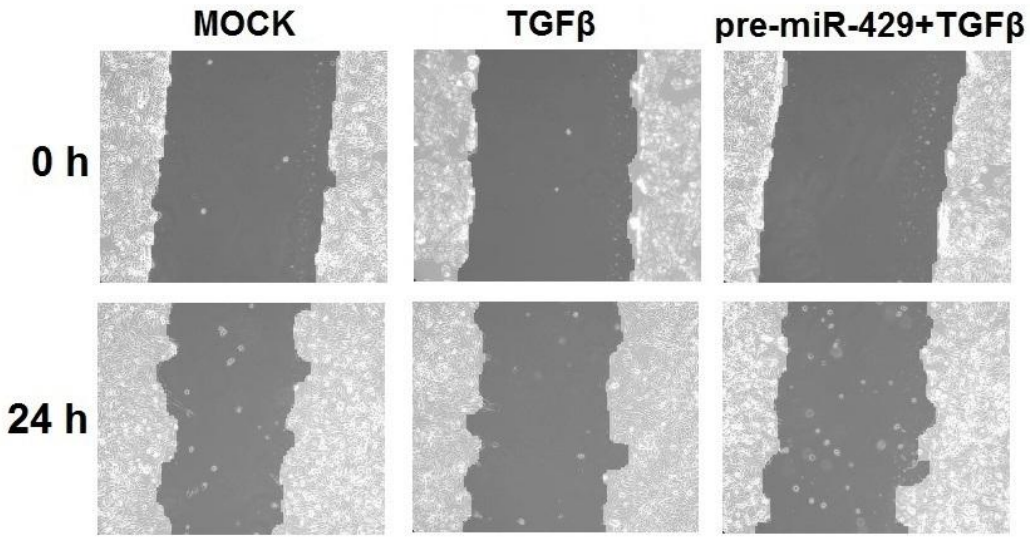

Figure 37: Images of ACHN cells transfected with negative control #1 (MOCK), cells treated with TGFβ and cells transfected with pre-miR-429 + treated with TGF β. 0h vs. 24h.

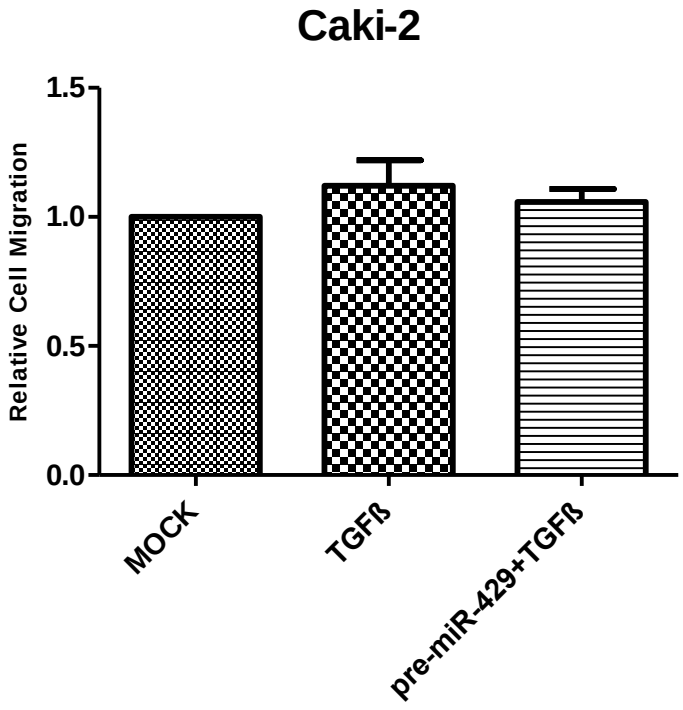

Figure 38: Relative cell migration of Caki-2 cells transfected with negative control #1 (MOCK), cells treated with TGFβ and cells transfected with pre-miR-429 + treated with TGF β.

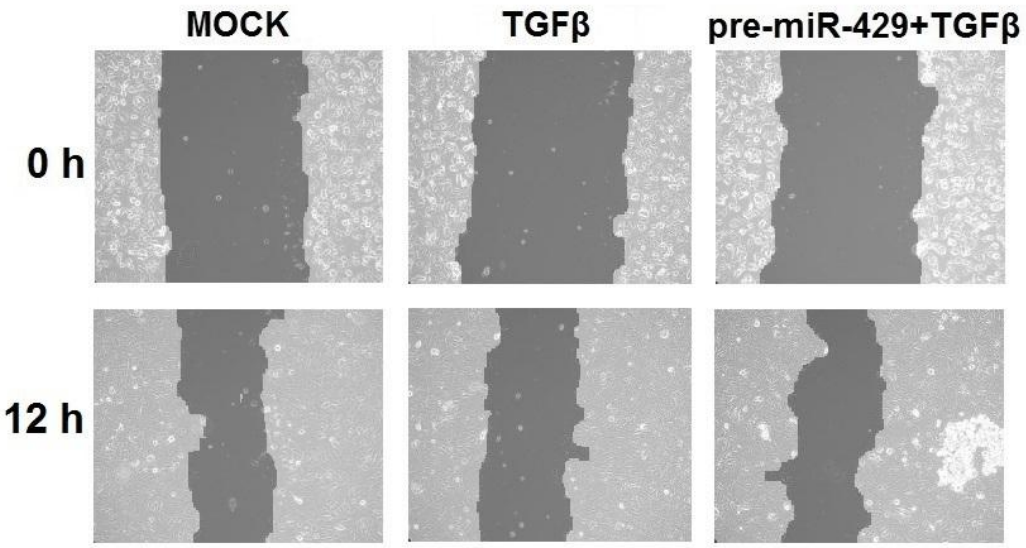

Figure 39: Images of Caki-2 cells transfected with negative control #1 (MOCK), cells treated with TGFβ and cells transfected with pre-miR-429 + treated with TGF β. 0h vs. 12h.

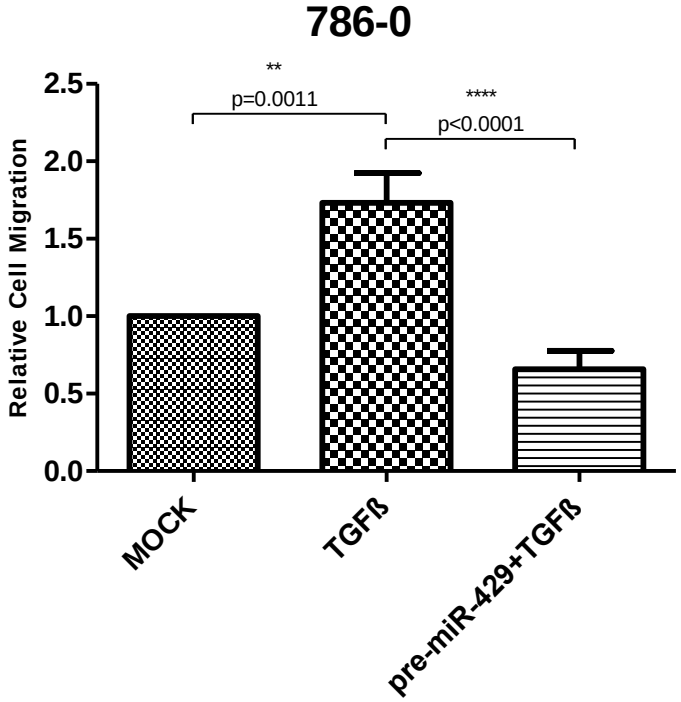

Figure 40: Relative cell migration of 786-0 cells transfected with negative control #1 (MOCK), cells treated with TGFβ and cells transfected with pre-miR-429 + treated with TGF β.

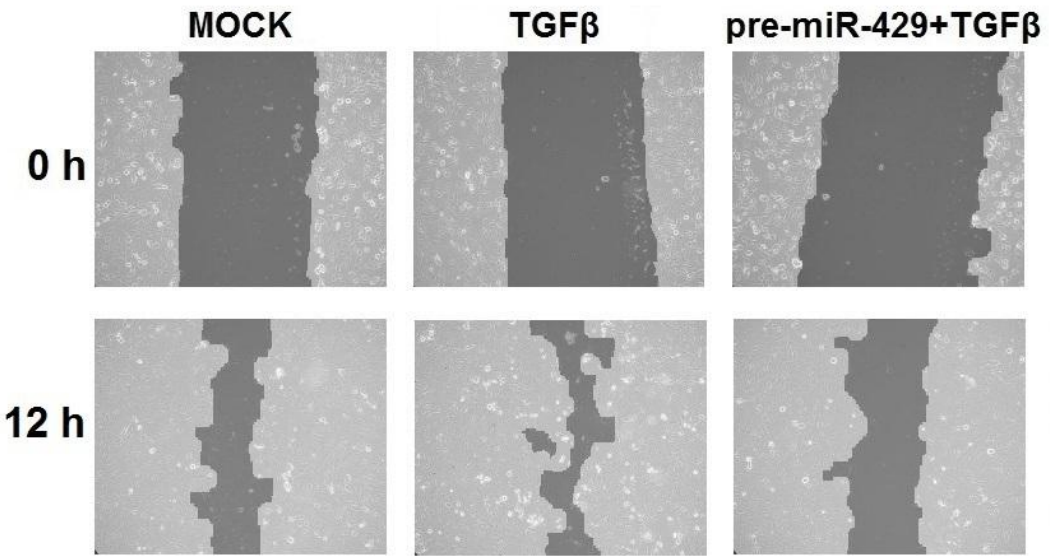

Figure 41: Images of 786-0 cells transfected with negative control #1 (MOCK), cells treated with TGFβ and cells transfected with pre-miR-429 + treated with TGF β. 0h vs. 12h.

5. Discussion

RCC is the most common neoplasm of renal parenchyma with the highest mortality rate of all genitourinary cancers. Czech Republic ranks with the highest incidence of RCC in the world [55]. RCC is a heterogeneous disease both in cellular morphology and clinical course of the disease. Heterogeneity is the problem that has been frequently associated with treatment failure [56]. RCC is classified into several subtypes from which ccRCC is the most common. Unfortunately, this disease is characterized by high chemo- and radio-resistance and early relapse after nephrectomy. Approximately 40% of all RCC patients with localized disease undergo relapse of the disease after surgical removal of the tumor. This high rate of recurrence for clinically localized disease after nephrectomy underscores the importance of post-surgical surveillance [57]. EMT is a multistep dynamic cellular phenomenon in which epithelial cells lose their cell–cell adhesion and gain migratory and invasive traits that are typical of mesenchymal cells. Other mesenchymal features include increased production of ECM components, resistance to apoptosis and ability to escape from immune system [58]. Initial step of EMT is a loss of E-cadherin, cell adhesion molecule. E-cadherin loss ostensibly promotes metastasis by enabling the first step of the metastatic cascade: the disaggregation of cancer cells from one another [59].

Since the first choice treatment of RCC is surgical removal of the tumor and then follow up of the patient, there is an urgent need for biomarkers that would be able to detect and predict metastasis in RCC patients. In recent years biomarker research has been oriented especially to non-coding RNAs and miRNAs among them. MicroRNAs are short 18-25 nucleotides long ncRNAs with outstanding stability even after several cycles of freezing and thawing. They can be detected by conventional methods like qRT-PCR, PCR, Northern Blot. MiRNAs have wide range of regulatory functions in cells and their expression is very often deregulated in tumor tissue in comparison to healthy tissue [60]. Moreover, miRNAs have been detected in body fluids (plasma, urine, saliva, tears, semen, cerebrospinal fluid, bronchial lavage, peritoneal fluid, pleural fluid, colostrum and breast milk). These circulating miRNAs have great potential as biomarkers in liquid biopsy [61,62]. Process of EMT is also accompanied by deregulation of several miRNAs. MiR-200 family includes five members (miR-200a, miR-200b, miR-200c, miR-141,

miR-429) and all of them are tumor suppressors targeting ZEB1 and ZEB2, transcriptional repressors of E-cadherin [63].

MiR-429 was chosen for validation after previous analyses in our laboratory using TLDA. EMT+ samples showed significantly downregulated miR-429 expression in comparison to EMT- samples. EMT+/EMT- status was determined immunohistochemically. In this study we validated expression of miR-429 in independent 231 samples (186 primary tumor tissues, 45 renal parenchyma tissues). Primary tumor tissue samples were further divided into three subgroups (no progression, progression and stage IV). MiR-429 was found to be significantly downregulated in primary tumor tissues in comparison to renal parenchyma tissues ($p<0.0001$). Moreover, miR-429 was significantly downregulated in primary tumor tissues of stage IV patients when compared to primary tumor tissues of patients with no progression ($p<0.0001$) and primary tumor tissues of patients with progression ($p=0.0115$) of RCC. Further, Kaplan-Meier survival analysis of miR-429 expression in primary tumor samples with/without progression showed that expression levels of miR-429 correlate with time to progression of the disease. Patients with higher expression levels of miR-429 in primary tumor tissue had significantly longer disease free survival than patients with lower expression levels of miR-429 in primary tumor tissue ($p=0.0105$). MiR-429 was previously reported to be downregulated in colorectal carcinoma (CRC) tissues and cell lines [64]. Another study reported significant downregulation of miR-429 expression in serum of patients with non-small lung cancer (NSLC) when compared to healthy serum. In addition, serum levels of miR-429 were associated with poor overall survival of NSCLC patients. Both univariate and multivariate analyses showed that serum miR-429 level was an independent prognostic predictor for NSCLC [65]. We can state that our observations correlated with results of previous studies of CRC and NSLC.

E-cadherin expression was measured in 231 RCC samples (186 primary tumor tissues, 45 renal parenchyma tissues) and primary tumor tissue samples were further divided into three subgroups (no progression, progression and stage IV). E-cadherin expression was found to be significantly downregulated in primary tumor tissues when compared to renal parenchyma tissues ($p<0.0001$). Downregulation of E-cadherin expression was also observed in primary tumor tissues of stage IV patients when compared to primary

tumor tissues of patients without progression ($p<0.0001$) and primary tumor tissues of patients with progression ($p=0.0100$). Kaplan-Meier survival analysis of E-cadherin expression in primary tumor tissues with/without progression did not prove any correlation between E-cadherin expression levels and DFS. E-cadherin is considered as a key molecule in EMT process; however, its expression is not consistent among various cancers. Different expression of E-cadherin was observed in primary breast cancer cells (BC) and invasive BC. Carcinomas *in situ* showed strong expression of E-cadherin while invasive carcinoma tissues without axillary lymph node metastases showed low expression of E-cadherin [66].

Induction of EMT by TGFβ was done in three RCC cell lines (ACHN, Caki-2, 786-0). Based on literature we used concentration 10 ng/ml of TGFβ. We evaluated effects of TGFβ on E-cadherin expression, cell metabolic activity and cell morphology. After TGFβ treatment decrease of E-cadherin expression was observed in all three cell lines. However, significant downregulation in E-cadherin expression was observed only in 786-0 cells treated with TGFβ in comparison to control cells both on day 2 ($p=0.0054$) and day 4 ($p=0.0053$). Downregulation of E-cadherin was previously reported in pancreatic cell lines PANC-1 and BXPC3 treated with TGFβ [67]**.** Another study reported upregulation of N-cadherin without change in E-cadherin expression after TGFβ treatment in ovarian cancer cell line NIH-OVCAR3 [68]. In this study we did not observe any relevant changes in cell morphology of ACHN and Caki-2 cell lines after TGFβ addition into the media. 786-0 cells appeared to be visibly longer and more spindle-shaped after TGFβ treatment. Previous evidence of TGFβ influence on cell morphology was observed in study of mouse mammary epithelial cells EpH4. In this study treatment of EpH4 cells by TGFβ resulted in unordered cell strands and cords with spindle-like cellular morphology [69]. Using MTT test we measured metabolic activity of ACHN, Caki-2 and 786-0 cells. Any significant differences in cell metabolic activity were not observed in all three cell lines. We can state that TGFβ does not affect metabolic activity of RCC cell lines ACHN, Caki-2 and 786-0. Effects of TGFβ on cell proliferation were described in several articles. For example in study from 2007 RCC bone metastasis (RBM) cells displayed either no change or decrease of metabolic activity after TGFβ treatment [70]. Another study of rat placental cells HRP-1 and RCHO-1 showed similar results. Decrease in proliferation was observed in HRP-1 cell line. On the other hand, no such a inhibitory effect was observed in RCHO-1 cell line [71].

Another task in functional studies was to find out the potential of miR-429 to repress effect of TGFβ on E-cadherin expression. We compared E-cadherin expression in cells transfected with negative control #1, cells transfected with pre-miR-429 + treated with TGFβ and cells treated with TGFβ. Any significant changes in E-cadherin expression between transfected/treated cells were not present. However, all three cell lines showed decreasing trend in E-cadherin expression in cells treated with TGFβ when compared to cells transfected with negative control #1 and most importantly to cells transfected with pre-miR-429 + treated with TGFβ. This results indicate effects of miR-429 on maintenance of E-cadherin expression during TGFβ-induced EMT. Effect of miR-200 family members on mainteinance of E-cadherin expression level during TGFβ-induced EMT were studied in several studies. Results vary dependently on miRNA and cell line [43,72,73].

Finally, we studied effect of miR-429 and TGFβ on cell migratory capacity. Cell lines ACHN and Caki-2 did not show any differences in relative cell migration after transfection with pre-miR-429/TGFβ treatment. Significant differences in relative cell migration were observed in 786-0 cell line. Cells treated with TGFβ migrated more than cells transfected with negative control #1 ($p=0.0011$) and cells transfected with pre-miR-429 + treated with TGFβ ($p<0.0001$). MiR-429 proved its potential to inhibit migratory capacity of 786-0 cells during TGFβ-induced EMT. Inhibition of cell migration by miR-200 members was previously reported. In study from 2008, overexpression of each member of the miR-200 clusters strongly reduced growth factor-induced directional migration of the mouse mammary tumor 4TO7 cells [74].

The above mentioned results prove that miR-429 is a tumor suppressor molecule involved in EMT regulation in RCC. MiR-429 and E-cadherin were significantly downregulated in RCC tissues in contrast to renal parenchyma tissues. Significant downregulation of miR-429 and E-cadherin was also observed in primary tumor tissues of stage IV patients in comparison to primary tumor tissues of patients without metastasis. Moreover, higher expression of miR-429 positively correlated with longer DFS of RCC patients.. Functional analyses on RCC cell lines showed that miR-429 has capacity to reverse E-cadherin repression and suppress enhanced cell migration during TGFβ-induced EMT in 786-0 cell line.

Summary

Introduction

Renal cell carcinoma is the most common neoplasm of renal parenchyma and accounts about 3% of all adult malignancies. Czech Republic ranks with the highest incidence of RCC in the world. RCC is characterized by high chemo- and radio-resistance and early relapse after nephrectomy. EMT is initial step of metastasis and cancer progression. Molecules involved in EMT regulation include, e.g. E-cadherin, ZEB1, ZEB2, TGFβ and miR-200 family.

Methods

Determination of miR-429 and E-cadherin expressions in 231 ccRCC samples was performed using qRT-PCR. *In vitro* analyses on three RCC cell lines (ACHN, Caki-2, 786-0) included TGFβ treatment, transient transfection (pre-miR-429), MTT test and scratch wound assay.

Results

Both miR-429 and E-cadherin were significantly downregulated in primary RCC tissues in comparison to renal parenchyma tissues ($p<0.0001$ and $p<0.0001$). Downregulation of miR-429 and E-cadherin was also observed in primary tumor tissues of stage IV patients when compared to primary tumor tissues of patients without progression ($p<0.0001$, $p<0.0001$) and with progression ($p=0.0115$, 0.0100). Higher expression of miR-429 positively correlated with longer DSF of RCC patients ($p=0.0105$). *In vitro* analyses showed that TGFβ treatment significantly decreases E-cadherin expression in 786-0 cell line (0.0053) and that miR-429 has ability to restore E-cadherin expression levels in RCC cell lines. Finally, miR-429 was able to suppress TGFβ-enhanced cell migratory capacity of 786-0 cell line ($p<0.0001$).

Conclusion

MiR-429 function as a tumor suppressor and is involved in regulation of EMT in RCC. In this study we found out that miR-429 and E-cadherin are significantly downregulated in RCC tissues in comparison to renal parenchyma tissues and significantly downregulated in primary RCC tissues of patients with metastasis in comparison to primary RCC tissues

of patients without metastasis. Furthermore, we upregulated miR-429 expression in three RCC cell lines and described its effects during TGFβ-induced EMT. We found out that miR-429 regulates E-cadherin expression levels and has capacity to repress cell migration of 786-0 cells during TGFβ-induced EMT. However, it would be needed to use stable transfection in order to analyze long term impact of miR-429 on other cellular processes.

References

[1] Ljungberg B, Campbell SC, Cho HY, Jacqmin D, Lee JE, Weikert S, et al. The Epidemiology of Renal Cell Carcinoma. Eur Urol 2011;60:615–21. doi:10.1016/j.eururo.2011.06.049.

[2] Terris M, Klaassen Z, Kabaria R. Renal cell carcinoma: links and risks. Int J Nephrol Renov Dis 2016:45. doi:10.2147/IJNRD.S75916.

[3] Chow W-H, Dong LM, Devesa SS. Epidemiology and risk factors for kidney cancer. Nat Rev Urol 2010;7:245–57. doi:10.1038/nrurol.2010.46.

[4] Dušek L, Mužík J, Kubásek M, Koptíková J, Žaloudík J, Vyzula R. Epidemiologie zhoubných nádorů v České republice [online]. Masaryk University 2005. Accesible from WWW: www.svod.cz. Version 7.0 2007, ISSN 1802-8861

[5] Protzel C, Maruschke M, Hakenberg OW. Epidemiology, Aetiology, and Pathogenesis of Renal Cell Carcinoma. Eur Urol Suppl 2012;11:52–9. doi:10.1016/j.eursup.2012.05.002.

[6] Colt JS, Schwartz K, Graubard BI, Davis F, Ruterbusch J, DiGaetano R, et al. Hypertension and Risk of Renal Cell Carcinoma Among White and Black Americans: Epidemiology 2011:1. doi:10.1097/EDE.0b013e3182300720.

[7] Audenet F, Yates DR, Cancel-Tassin G, Cussenot O, Rouprêt M. Genetic pathways involved in carcinogenesis of clear cell renal cell carcinoma: genomics towards personalized medicine: CARCINOGENESIS OF CLEAR CELL RENAL CELL CARCINOMA. Bju Int 2012;109:1864–70. doi:10.1111/j.1464-410X.2011.10661.x.

[8] Cowey CL, Rathmell WK. VHL gene mutations in renal cell carcinoma: Role as a biomarker of disease outcome and drug efficacy. Curr Oncol Rep 2009;11:94–101. doi:10.1007/s11912-009-0015-5.

[9] Stehle F, Leisz S, Schulz K. VHL-dependent alterations in the secretome of renal cell carcinoma: Association with immune cell response? Oncotarget 2015. doi:10.18632/oncotarget.5560.

[10] Banumathy G, Cairns P. Signaling pathways in renal cell carcinoma. Cancer Biol Ther 2010;10:658–64. doi:10.4161/cbt.10.7.13247.

[11] Patel PH, Chaganti RSK, Motzer RJ. Targeted therapy for metastatic renal cell carcinoma. Br J Cancer 2006, 94(5):614-619. doi:10.1038/sj.bjc.6602978.

[12] Kalluri R, Weinberg RA. The basics of epithelial-mesenchymal transition. J Clin Invest 2009;119:1420–8. doi:10.1172/JCI39104.

[13] Shiota M, Zardan A, Takeuchi A, Kumano M, Beraldi E, Naito S, et al. Clusterin Mediates TGF- -Induced Epithelial-Mesenchymal Transition and Metastasis via Twist1 in Prostate Cancer Cells. Cancer Res 2012;72:5261–72. doi:10.1158/0008-5472.CAN-12-0254.

[14] Kim Y-S, Yi B-R, Kim N-H, Choi K-C. Role of the epithelial–mesenchymal transition and its effects on embryonic stem cells. Exp Mol Med 2014;46:e108. doi:10.1038/emm.2014.44.

[15] Kalluri R. EMT: When epithelial cells decide to become mesenchymal-like cells. J Clin Invest 2009;119:1417–9. doi:10.1172/JCI39675.

[16] Wynn TA, Ramalingam TR. Mechanisms of fibrosis: therapeutic translation for fibrotic disease. Nat Med 2012;18:1028–40. doi:10.1038/nm.2807.

[17] Heerboth S, Housman G, Leary M, Longacre M, Byler S, Lapinska K, et al. EMT and tumor metastasis. Clin Transl Med 2015;4. doi:10.1186/s40169-015-0048-3.

[18] Scheel C, Weinberg RA. Cancer stem cells and epithelial–mesenchymal transition: Concepts and molecular links. Semin Cancer Biol 2012;22:396–403. doi:10.1016/j.semcancer.2012.04.001.

[19] Fabregat I, Malfettone A, Soukupova J. New Insights into the Crossroads between EMT and Stemness in the Context of Cancer. J Clin Med 2016;5:37. doi:10.3390/jcm5030037.

[20] Larue L, Bellacosa A. Epithelial–mesenchymal transition in development and cancer: role of phosphatidylinositol 3′ kinase/AKT pathways. Oncogene 2005;24:7443–54. doi:10.1038/sj.onc.1209091.

[21] Fujita Y, Hogan C. Adherens Junction. Encycl. Ref. Genomics Proteomics Mol. Med., Berlin, Heidelberg: Springer Berlin Heidelberg; 2006, p. 20–5.

[22] Wheelock MJ, Shintani Y, Maeda M, Fukumoto Y, Johnson KR. Cadherin switching. J Cell Sci 2008;121:727–35. doi:10.1242/jcs.000455.

[23] Jeanes A, Gottardi CJ, Yap AS. Cadherins and cancer: how does cadherin dysfunction promote tumor progression? Oncogene 2008;27:6920–9. doi:10.1038/onc.2008.343.

[24] Sun B, Fang Y, Li Z, Chen Z, Xiang J. Role of cellular cytoskeleton in epithelial-mesenchymal transition process during cancer progression (Review). Biomed Reports 2015. doi:10.3892/br.2015.494.

[25] Puisieux A, Brabletz T, Caramel J. Oncogenic roles of EMT-inducing transcription factors. Nat Cell Biol 2014;16:488–94. doi:10.1038/ncb2976.

[26] Lamouille S, Xu J, Derynck R. Molecular mechanisms of epithelial–mesenchymal transition. Nat Rev Mol Cell Biol 2014;15:178–96. doi:10.1038/nrm3758.

[27] Craene BD, Berx G. Regulatory networks defining EMT during cancer initiation and progression. Nat Rev Cancer 2013;13:97–110. doi:10.1038/nrc3447.

[28] Barrallo-Gimeno A. The Snail genes as inducers of cell movement and survival: implications in development and cancer. Development 2005;132:3151–61. doi:10.1242/dev.01907.

[29] Sánchez-Tilló E, Siles L, de Barrios O, Cuatrecasas M, Vaquero EC, Castells A, et al. Expanding roles of ZEB factors in tumorigenesis and tumor progression. Am J Cancer Res 2011;1:897–912.

[30] Isenmann S, Arthur A, Zannettino AC, Turner JL, Shi S, Glackin CA, et al. TWIST Family of Basic Helix-Loop-Helix Transcription Factors Mediate Human Mesenchymal Stem Cell Growth and Commitment. Stem Cells 2009;27:2457–68. doi:10.1002/stem.181.

[31] Fendrich V, Waldmann J, Feldmann G, Schlosser K, Konig A, Ramaswamy A, et al. Unique expression pattern of the EMT markers Snail, Twist and E-cadherin in benign and malignant parathyroid neoplasia. Eur J Endocrinol 2009;160:695–703. doi:10.1530/EJE-08-0662.

[32] Serrano-Gomez SJ, Maziveyi M, Alahari SK. Regulation of epithelial-mesenchymal transition through epigenetic and post-translational modifications. Mol Cancer 2016;15. doi:10.1186/s12943-016-0502-x.

[33] Ha M, Kim VN. Regulation of microRNA biogenesis. Nat Rev Mol Cell Biol 2014;15:509–24. doi:10.1038/nrm3838.

[34] Winter J, Jung S, Keller S, Gregory RI, Diederichs S. Many roads to maturity: microRNA biogenesis pathways and their regulation. Nat Cell Biol 2009;11:228–34. doi:10.1038/ncb0309-228.

[35] Denli AM, Tops BBJ, Plasterk RHA, Ketting RF, Hannon GJ. Processing of primary microRNAs by the Microprocessor complex. Nature 2004;432:231–5. doi:10.1038/nature03049.

[36] Yi R. Exportin-5 mediates the nuclear export of pre-microRNAs and short hairpin RNAs. Genes Dev 2003;17:3011–6. doi:10.1101/gad.1158803.

[37] Chendrimada TP, Gregory RI, Kumaraswamy E, Norman J, Cooch N, Nishikura K, et al. TRBP recruits the Dicer complex to Ago2 for microRNA processing and gene silencing. Nature 2005;436:740–4. doi:10.1038/nature03868.

[38] Havens MA, Reich AA, Duelli DM, Hastings ML. Biogenesis of mammalian microRNAs by a non-canonical processing pathway. Nucleic Acids Res 2012;40:4626–40. doi:10.1093/nar/gks026.

[39] Barh D, Malhotra R, Ravi B, Sindhurani P. Microrna let-7: an emerging next-generation cancer therapeutic. Curr Oncol 2010;17. doi:10.3747/co.v17i1.356.

[40] Gregory PA, Bert AG, Paterson EL, Barry SC, Tsykin A, Farshid G, et al. The miR-200 family and miR-205 regulate epithelial to mesenchymal transition by targeting ZEB1 and SIP1. Nat Cell Biol 2008;10:593–601. doi:10.1038/ncb1722.

[41] Lamouille S, Subramanyam D, Blelloch R, Derynck R. Regulation of epithelial–mesenchymal and mesenchymal–epithelial transitions by microRNAs. Curr Opin Cell Biol 2013;25:200–7. doi:10.1016/j.ceb.2013.01.008.

[42] Korpal M, Lee ES, Hu G, Kang Y. The miR-200 Family Inhibits Epithelial-Mesenchymal Transition and Cancer Cell Migration by Direct Targeting of E-cadherin Transcriptional Repressors ZEB1 and ZEB2. J Biol Chem 2008;283:14910–4. doi:10.1074/jbc.C800074200.

[43] Park S-M, Gaur AB, Lengyel E, Peter ME. The miR-200 family determines the epithelial phenotype of cancer cells by targeting the E-cadherin repressors ZEB1 and ZEB2. Genes Dev 2008;22:894–907. doi:10.1101/gad.1640608.

[44] Burk U, Schubert J, Wellner U, Schmalhofer O, Vincan E, Spaderna S, et al. A reciprocal repression between ZEB1 and members of the miR-200 family promotes EMT and invasion in cancer cells. EMBO Rep 2008;9:582–9. doi:10.1038/embor.2008.74.

[45] Mutlu M, Saatçi ö, Raza U, Eyüpoglu E, Yurdusev E, Sahin ö. MIR200C (microRNA 200c). Atlas Genet Cytogenet Oncol Haematol 2015. doi:10.4267/2042/56438.

[46] McCaffrey LM, Macara IG. Epithelial organization, cell polarity and tumorigenesis. Trends Cell Biol 2011;21:727–35. doi:10.1016/j.tcb.2011.06.005.

[47] Muralidhar G, Barbolina M. The miR-200 Family: Versatile Players in Epithelial Ovarian Cancer. Int J Mol Sci 2015;16:16833–47. doi:10.3390/ijms160816833.

[48] Mao Y, Wu S, Zhao R, Deng Q. MiR-205 promotes proliferation, migration and invasion of nasopharyngeal carcinoma cells by activation of AKT signalling. J Int Med Res 2016;44:231–40. doi:10.1177/0300060515576556.

[49] Piovan C, Palmieri D, Di Leva G, Braccioli L, Casalini P, Nuovo G, et al. Oncosuppressive role of p53-induced miR-205 in triple negative breast cancer. Mol Oncol 2012;6:458–72. doi:10.1016/j.molonc.2012.03.003.

[50] Zhang P, Wang L, Rodriguez-Aguayo C, Yuan Y, Debeb BG, Chen D, et al. miR-205 acts as a tumour radiosensitizer by targeting ZEB1 and Ubc13. Nat Commun 2014;5:5671. doi:10.1038/ncomms6671.

[51] Wiklund ED, Bramsen JB, Hulf T, Dyrskjøt L, Ramanathan R, Hansen TB, et al. Coordinated epigenetic repression of the miR-200 family and miR-205 in invasive bladder cancer. Int J Cancer 2011;128:1327–34. doi:10.1002/ijc.25461.

[52] Wang B, Herman-Edelstein M, Koh P, Burns W, Jandeleit-Dahm K, Watson A, et al. E-Cadherin Expression Is Regulated by miR-192/215 by a Mechanism That Is Independent of the Profibrotic Effects of Transforming Growth Factor-. Diabetes 2010;59:1794–802. doi:10.2337/db09-1736.

[53] Boni V, Bitarte N, Cristobal I, Zarate R, Rodriguez J, Maiello E, et al. miR-192/miR-215 Influence 5-Fluorouracil Resistance through Cell Cycle-Mediated Mechanisms Complementary to Its Post-transcriptional Thymidilate Synthase Regulation. Mol Cancer Ther 2010;9:2265–75. doi:10.1158/1535-7163.MCT-10-0061.

[54] Mu J, Pang Q, Guo Y-H, Chen J-G, Zeng W, Huang Y-J, et al. Functional Implications of MicroRNA-215 in TGF-β1-Induced Phenotypic Transition of Mesangial Cells by Targeting CTNNBIP1. Plos One 2013;8:e58622. doi:10.1371/journal.pone.0058622.

[55] Paul C. Renal cell carcinoma. Cancer Biomark 2011:461–73. doi:10.3233/CBM-2011-0176.

[56] Vaziri SAJ, Ganapathi MK, Ganapathi RN. Genetic Heterogeneity in Renal Cell Carcinoma: Clinical Implications? In: Bukowski RM, Figlin RA, Motzer RJ, editors. Ren. Cell Carcinoma, New York, NY: Springer New York; 2015, p. 167–76.

[57] Stewart-Merrill SB, Thompson RH, Boorjian SA, Psutka SP, Lohse CM, Cheville JC, et al. Oncologic Surveillance After Surgical Resection for Renal Cell Carcinoma: A Novel Risk-Based Approach. J Clin Oncol 2015;33:4151–7. doi:10.1200/JCO.2015.61.8009.

[58] Grigore A, Jolly M, Jia D, Farach-Carson M, Levine H. Tumor Budding: The Name is EMT. Partial EMT. J Clin Med 2016;5:51. doi:10.3390/jcm5050051.

[59] Onder TT, Gupta PB, Mani SA, Yang J, Lander ES, Weinberg RA. Loss of E-Cadherin Promotes Metastasis via Multiple Downstream Transcriptional Pathways. Cancer Res 2008;68:3645–54. doi:10.1158/0008-5472.CAN-07-2938.

[60] Van Roosbroeck K, Pollet J, Calin GA. miRNAs and long noncoding RNAs as biomarkers in human diseases. Expert Rev Mol Diagn 2013;13:183–204. doi:10.1586/erm.12.134.

[61] Weber JA, Baxter DH, Zhang S, Huang DY, How Huang K, Jen Lee M, et al. The MicroRNA Spectrum in 12 Body Fluids. Clin Chem 2010;56:1733–41. doi:10.1373/clinchem.2010.147405.

[62] Creemers EE, Tijsen AJ, Pinto YM. Circulating MicroRNAs: Novel Biomarkers and Extracellular Communicators in Cardiovascular Disease? Circ Res 2012;110:483–95. doi:10.1161/CIRCRESAHA.111.247452.

[63] Chan S-H, Wang L-H. Regulation of cancer metastasis by microRNAs. J Biomed Sci 2015;22:9. doi:10.1186/s12929-015-0113-7.

[64] Sun Y, Shen S, Liu X, Tang H, Wang Z, Yu Z, et al. miR-429 inhibits cells growth and invasion and regulates EMT-related marker genes by targeting Onecut2 in colorectal carcinoma. Mol Cell Biochem 2014;390:19–30. doi:10.1007/s11010-013-1950-x.

[65] Zhu W, He J, Chen D, Zhang B, Xu L, Ma H, et al. Expression of miR-29c, miR-93, and miR-429 as Potential Biomarkers for Detection of Early Stage Non-Small Lung Cancer. Plos One 2014;9:e87780. doi:10.1371/journal.pone.0087780.

[66] Jeschke U, Mylonas I, Kuhn C, Shabani N, Kunert-Keil C, Schindlbeck C, et al. Expression of E-cadherin in human ductal breast cancer carcinoma in situ, invasive carcinomas, their lymph node metastases, their distant metastases, carcinomas with recurrence and in recurrence. Anticancer Res 2007;27:1969–74.

[67] Vogelmann R. TGF -induced downregulation of E-cadherin-based cell-cell adhesion depends on PI3-kinase and PTEN. J Cell Sci 2005;118:4901–12. doi:10.1242/jcs.02594.

[68] Gao J, Zhu Y, Nilsson M, Sundfeldt K. TGF-β isoforms induce EMT independent migration of ovarian cancer cells. Cancer Cell Int 2014;14. doi:10.1186/s12935-014-0072-1.

[69] Janda E, Lehmann K, Killisch I, Jechlinger M, Herzig M, Downward J, et al. Ras and TGFβ cooperatively regulate epithelial cell plasticity and metastasis: dissection of Ras signaling pathways. J Cell Biol 2002;156:299–314. doi:10.1083/jcb.200109037.

[70] Kominsky SL, Doucet M, Brady K, Weber KL. TGF-beta promotes the establishment of renal cell carcinoma bone metastasis. J Bone Miner Res Off J Am Soc Bone Miner Res 2007;22:37–44. doi:10.1359/jbmr.061005.

[71] Lafontaine L, Chaudhry P, Lafleur M-J, Van Themsche C, Soares MJ, Asselin E. Transforming Growth Factor Beta Regulates Proliferation and Invasion of Rat Placental Cell Lines. Biol Reprod 2011;84:553–9. doi:10.1095/biolreprod.110.086348.

[72] Chen Y, Xiao Y, Ge W, Zhou K, Wen J, Yan W, et al. miR-200b inhibits TGF-β1-induced epithelial-mesenchymal transition and promotes growth of intestinal epithelial cells. Cell Death Dis 2013;4:e541. doi:10.1038/cddis.2013.22.

[73] Wu C-L, Ho J-Y, Chou S-C, Yu D-S. MiR-429 reverses epithelial-mesenchymal transition by restoring E-cadherin expression in bladder cancer. Oncotarget 2016. doi:10.18632/oncotarget.8557.

[74] Korpal M, Lee ES, Hu G, Kang Y. The miR-200 Family Inhibits Epithelial-Mesenchymal Transition and Cancer Cell Migration by Direct Targeting of E-cadherin Transcriptional Repressors ZEB1 and ZEB2. J Biol Chem 2008;283:14910–4. doi:10.1074/jbc.C800074200.